

Catch me if you can: Signal localization with knockoff e-values

Paula Gablenz¹ and Chiara Sabatti^{2,1}

¹Department of Statistics, Stanford University

²Department of Biomedical Data Science, Stanford University

Abstract

We consider problems where many, somewhat redundant, hypotheses are tested and we are interested in reporting the most precise rejections, with false discovery rate (FDR) control. This is the case, for example, when researchers are interested both in individual hypotheses as well as group hypotheses corresponding to intersections of sets of the original hypotheses, at several resolution levels. A concrete application is in genome-wide association studies, where, depending on the signal strengths, it might be possible to resolve the influence of individual genetic variants on a phenotype with greater or lower precision. To adapt to the unknown signal strength, analyses are conducted at multiple resolutions and researchers are most interested in the more precise discoveries. Assuring FDR control on the reported findings with these adaptive searches is, however, often impossible. To design a multiple comparison procedure that allows for an adaptive choice of resolution with FDR control, we leverage e-values and linear programming. We adapt this approach to problems where knockoffs and group knockoffs have been successfully applied to test conditional independence hypotheses. We demonstrate its efficacy by analyzing data from the UK Biobank.

Keywords: FDR, grouped hypotheses, GWAS, knockoffs, multiple testing, multiple resolutions.

1 Introduction

Finding, among many features, those that contain information on an outcome of interest is an important statistical problem which can be described in terms of testing multiple conditional independence hypotheses. For example, genome wide association studies (GWAS) are devoted to identifying single nucleotide polymorphisms (SNPs) whose alleles influence a medically relevant phenotype Y . A discovered SNP is truly interesting when it provides information on Y in addition to that available in the rest of the genome. For each polymorphism j in the

study, a conditional independence hypothesis can be written as

$$H_j : Y \perp\!\!\!\perp \text{SNP}_j \mid \text{SNP}_{-j} \quad (1)$$

with $j \in \{1, \dots, p\}$ and where SNP_{-j} denotes all SNPs except SNP_j . The process with which we inherit genetic material from our parents is such that, within a human population, the random variables describing alleles at SNPs located in proximity of each other along a chromosome are dependent. This local dependency, known as linkage disequilibrium, can make it difficult to reject hypotheses of the type of (1), as the variation in each SNP is typically well recapitulated by its neighbors. To avoid power loss, it is convenient to test conditional hypotheses corresponding to groups of highly correlated SNPs. This is, for example, the solution adopted in [Sesia et al. \(2020\)](#), where hierarchical clustering is used to define multiple groupings of SNPs, corresponding to different correlation thresholds: conditional testing with false discovery rate (FDR) control is carried out for each of these partitions in the genome, resulting in discoveries at multiple resolutions, as the one illustrated in the top panel of [Figure 1](#).

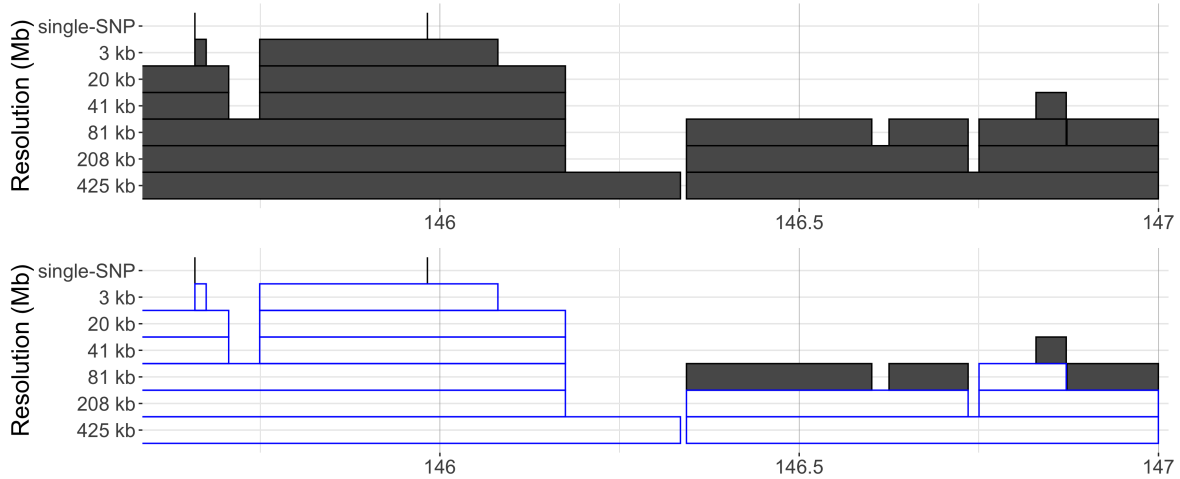


Figure 1: Examples of the results of the analysis of height in the UK Biobank ([Sesia et al., 2020](#)). Genomic position is on the x -axis (this is a small portion of chromosome 4). Different heights on the y -axis correspond to different resolutions. Top panel: Each filled gray box corresponds to a group of SNPs for which the hypothesis of independence from height given the rest of the genome has been rejected, carrying out an analysis that controls FDR at each resolution ([Sesia et al., 2020](#)). Lower panel: the most specific discoveries among those in the top panel are highlighted as filled gray boxes, while the others (logically implied) are empty rectangles.

Scientists, presented with these results, are interested in focusing on the most precise discoveries, highlighted in the bottom panel of [Figure 1](#). However, such post-hoc selection of

non redundant findings breaks FDR guarantees provided by the original algorithm (Katsevich et al., 2021). This limitation of FDR procedures is well known (Goeman and Solari, 2011) and is one reason that makes alternative approaches more attractive, despite possible loss of power (for example, in the context of genetic analysis; see the contribution by Renaux et al. (2020) and related discussion papers). Another line of work for controlling false discoveries by providing upper confidence bounds on the number of false discoveries has been developed by Genovese and Wasserman (2004); Goeman and Solari (2011); Goeman et al. (2019) and extended to e-values by Vovk and Wang (2023).

GWAS are but one example of what one might call “resolution adaptive” testing: problems where scientists are aiming to simultaneously discover a signal and localize it as precisely as possible (Spector and Janson, 2023). Localization might refer to a physical position in the genome or in space (Rosenblatt et al., 2018), but it can also more broadly be construed as precision of the finding: in Cortes et al. (2017), for example, localizing a signal corresponds to identifying the nodes farther from the root in a tree describing a set of related diseases. There is typically a tension between the precision of a discovery and the ability to detect the underlying signal: scientists are interested in finding the most high resolution at which interesting rejections can be made. When the space of hypotheses explored is very large, it is reasonable to expect that this “optimal” resolution might vary across the existing signals. At the same time, the adaptive selection of resolution is complicated by the need to account for multiplicity, providing some global error guarantees.

The literature documents multiple approaches to tackling this problem. Without attempting a comprehensive review, it is worth pointing out that they vary with respect to target error rate (ex. FWER or FDR), and the assumptions they make on the relation between hypotheses at different levels of resolution. For example, Meijer and Goeman (2015) develop a sequential multiple testing method to control the FWER for hypotheses that can be described by a directed acyclic graph and they are able to increase power by leveraging logical relations between hypotheses. A similar setting is considered in Ramdas et al. (2019a), which targets FDR control. In this work, we consider settings where no restriction is placed on the hypotheses at different resolutions (for example, we do not require partitions to be nested). This allows us to model situations where the different resolutions capture different, possibly quite unrelated, procedures to query the data.

Spector and Janson (2023) recently studied this problem. Following Mandozzi and Bühlmann (2016), they provide a clear formalization of the tension between localization and discovery and give an elegant and efficient solution in a Bayesian framework (BLiP). While guarantees on the Bayesian FDR are a useful step forward, when posterior probabilities for each of the tested hypotheses are available, they are not satisfactory for a large portion of the scientific community who finds the frequentist approach to inference an easier platform for agreement.

Working in a frequentist framework, Katsevich et al. (2021) considered a larger class of multi-

ple testing problems where researchers might be interested in refining the set of discoveries to eliminate redundancy, broadly defined. They introduce a multiple testing procedure (Focused BH) that generalizes the Benjamini and Hochberg (BH) procedure (Benjamini and Hochberg, 1995), and controls the FDR when the p-values for all hypotheses considered are independent or have a special type of positive dependence called PRDS (Positive Regression Dependency on each one from a Subset) (Benjamini and Yekutieli, 2001b). Given the complex dependence structure of tests build on overlapping/nested sets of predictors as the ones in GWAS, these distributional assumptions are limiting, and the extension of Focused BH described in Katsevich et al. (2021) to arbitrary filters and dependency structures is very conservative.

An example of special interest is the multi resolution analysis of GWAS data with conditional hypotheses (Sesia et al., 2020) enabled by the knockoff framework (Barber and Candès, 2015; Candès et al., 2018) illustrated in Figure 1. Here the p-values are dependent and they are designed to be analyzed with a special multiple comparison adjustment procedure that is not captured by Focused BH.

To address this gap, we introduce a resolution-adaptive, multiple comparison procedure that leads to frequentist FDR control without making distributional assumptions on the test statistics. A key ingredient to our approach are e-values, and their “easy” calculus (Vovk and Wang, 2021; Wang and Ramdas, 2022). Working with e-values, we can define a linear program related to that one in Spector and Janson (2023) and leading to frequentist FDR control.

These results are concretely interesting because we can describe powerful e-values for resolution adaptive variable selection. Ren and Barber (2023) have recently shown how the knockoff filter can be re-interpreted as a BH-type procedure (Wang and Ramdas, 2022) on specially constructed e-values. Building on their work, we introduce KeLP (Knockoff e-value Linear Program), with which we can analyze genomescale data in a powerful and time-efficient manner.

The rest of the paper is organized as follows. We formally introduce the problem in section 2, describe a solution using e-values in section 3, and operationalize it for testing conditional hypotheses with knockoffs in section 4. We describe additional applications of KeLP in section 5. Section 6 is devoted to simulations and Section 7 presents the results of applying our methods to the UK Biobank data.

2 Problem statement and notation

We consider problems where investigators are interested in evaluating p null hypotheses $\{H_1, \dots, H_p\}$ as well as “group” hypotheses, which correspond to intersections of the original ones. An individual hypothesis can contribute to the definition of multiple group hypotheses, corresponding to different levels of resolution. For example, functional magnetic resonance imaging (fMRI) studies measure millions of voxels at different time intervals. While the most

precise hypotheses that can be investigated describe the behavior of one voxel at one time point, scientists are also interested in aggregating the signal to correspond to larger structures and time frames.

Formally, let \mathcal{M} denote a set of resolutions and \mathcal{A}^m denote a partition of $\{1, \dots, p\}$ into disjoint groups at resolution $m \in \mathcal{M}$. With $A_g^m \in \mathcal{A}^m$ for $g \in \{1, \dots, |\mathcal{A}^m|\}$ we indicate the elements of the partition \mathcal{A}^m , each of which is a disjoint set of indices $j \in \{1, \dots, p\}$, which we refer to as a group.

Each group defines a hypothesis

$$H_g^m = \bigcap_{j \in A_g^m} H_j \quad \text{for all } g, m. \quad (2)$$

To avoid confusion, we use $m = 1$ to indicate the partition \mathcal{A}^1 of $\{1, \dots, p\}$ into p sets of size 1, so that $H_j^1 = H_j$ for $j = 1, \dots, p$. Referring to the index m as a resolution, we underscore how the various partitions have a different degree of coarseness; however, we do not require that the partitions are nested, nor that there is a natural ordering among them. Let \mathcal{H}^m denote the set of resolution-specific hypotheses for $m \in \mathcal{M}$ and \mathcal{H}_0^m the corresponding set of true nulls. Combining several levels of resolution, let $\mathcal{H} = \{\mathcal{H}^m\}_{m \in \mathcal{M}}$ denote the combined set of hypotheses across resolutions and $\mathcal{H}_0 = \{\mathcal{H}_0^m\}_{m \in \mathcal{M}}$ the combined set of true null hypotheses. We also let $\mathcal{A} = \{\mathcal{A}^m\}_{m \in \mathcal{M}}$ denote the set of groups across all levels of resolution. For simplicity of notation, we will let a group in \mathcal{A} be denoted as $A \in \mathcal{A}$ with the understanding that these groups are of course resolution-specific. To each group $A \in \mathcal{A}$ corresponds an hypothesis $H_A \in \mathcal{H}$, for which we have a valid test (as described further in sections 3 and 4, we will work with e-values). Figure 2 gives a schematic illustration of a multi-resolution family of hypotheses \mathcal{H} .

When the size of these families is large, it is necessary to control some measure of global error and in many scientific settings the false discovery rate (Benjamini and Hochberg, 1995) is often a preferred choice. Given the structure of the multi-resolution families, however, there are multiple ways of defining the FDR: one can consider the total collection of rejections across resolutions, and control the expected value of the false discovery proportion among them; or one can control the FDR within each resolution separately - possibly enforcing consistency across resolutions; or one might want to focus on the most precise discoveries made (the ones indicated with a blue thick contour in Figure 2) and control the FDR among them.

All of these choices are documented in the literature. For example, as anticipated, Knockoff-Zoom (Sesia et al., 2020) controls the FDR separately within each resolution; the p-filter (Barber and Ramdas, 2017) and the Multilayer Knockoff Filter (MKF) (Katsevich and Sabatti, 2019) result in coordinated discoveries across resolutions, with simultaneous FDR control within each resolution. The most precise discoveries have been described as “outer-nodes”

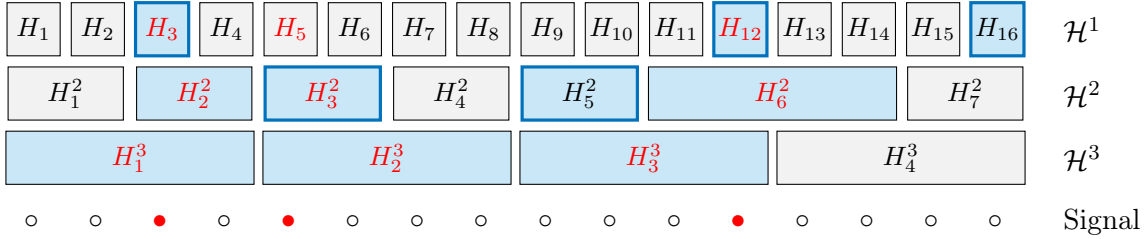


Figure 2: Schematic representation of a multi-resolution family of hypotheses $\mathcal{H} = \{\mathcal{H}^1, \mathcal{H}^2, \mathcal{H}^3\}$ and a rejection set \mathcal{R} . Resolution 1 corresponds to individual level hypotheses; resolutions 2 and 3 correspond to two different partitions of the 16 hypotheses. False null hypotheses are indicated in red and capture the underlying signal at different resolutions. The hypotheses part of the rejection set \mathcal{R} are shaded in blue; the most specific rejections are highlighted with thick blue contours. The overall FDP is $2/10$. The FDP for resolution 1 is $1/3$; for resolution 2 the FDP is $1/4$, and for resolution 3, the FDP is 0. The FDP for the set of non-redundant and most precise discoveries is $2/5$.

when the partitions corresponding to different resolutions are nested and the tested hypotheses can be organized in a hierarchical tree structure: Yekutieli (2008) proves the first result of FDR control in this framework, under some restrictive assumptions. Mandozzi and Bühlmann (2016) tackle the problem from the point of view of Family Wise Error Rate (FWER). Both BLiP (Spector and Janson, 2023) and Focused BH (Katsevich et al., 2021) consider approaches to identify non-redundant and precise rejection sets and develop methodology that leads to FDR control in some settings. This is also our goal.

Specifically, let \mathcal{F} be a multiple testing procedure applied to \mathcal{H} that outputs a rejection set $\mathcal{R}_{\mathcal{F}}$. Let $\mathcal{A}_{\mathcal{R}_{\mathcal{F}}} = \{A \text{ s.t. } H_A \in \mathcal{R}_{\mathcal{F}}\}$. We define the rejections $\mathcal{R}_{\mathcal{F}}$ to be non-redundant if $\mathcal{A}_{\mathcal{R}_{\mathcal{F}}}$ contains disjoint sets. As in Mandozzi and Bühlmann (2016), we are interested in “minimal” non-redundant discoveries, that is those corresponding to the groups with the smallest cardinality; at the same time, as in Spector and Janson (2023), we do not want to restrict ourselves to nested partitions. To capture the value of rejecting a particular hypothesis H_A , we use weights $w(A)$, as in Spector and Janson (2023); in particular we often focus on the original suggestion in Mandozzi and Bühlmann (2016) with $w(A) = 1/|A|$, where $|A|$ is the cardinality of A . The following formalizes our goal of finding a multiple testing procedure which maximizes the resolution-adjusted rejection count, controlling the FDR and leading to non-redundant findings.

Goal. Resolution-adaptive discovery with FDR control. *Given a multi-resolution family of hypotheses \mathcal{H} as described above, corresponding to a collection of groups \mathcal{A} ; a fixed weighting function $w : \mathcal{A} \rightarrow \mathbb{R}^+$, capturing the value of discoveries at different resolutions; and a level $\alpha \in (0, 1)$ of desired FDR, we seek a multiple testing procedure \mathcal{F} which solves the*

following constrained optimization problem:

$$\max \sum_{A \in \mathcal{A}_{\mathcal{R}_{\mathcal{F}}}} w(A) \tag{3}$$

$$s.t. \quad FDR(\mathcal{F}) = \mathbb{E} \left[\frac{|\mathcal{R}_{\mathcal{F}} \cap \mathcal{H}_0|}{1 \vee |\mathcal{R}_{\mathcal{F}}|} \right] \leq \alpha \tag{4}$$

$$A, B \in \mathcal{A}_{\mathcal{R}_{\mathcal{F}}} \Rightarrow A \cap B = \emptyset \tag{5}$$

Before introducing a procedure that solves this problem, we pause to make a few remarks. First, in contrast to [Spector and Janson \(2023\)](#), who use posterior probabilities to maximize a notion of expected power, our objective (3) is to maximize the number of (weighted) rejections: we want the largest number of valuable discoveries, while controlling FDR.

Second, while we focus on situations where the value of discoveries is described by weights $w(A)$ decreasing in $|A|$, in different contexts it might be useful to consider other evaluations: the procedures we will describe adapt to any, as long as the weights are fixed.

The constraint (5) expresses our interest in obtaining non-redundant rejections. In section 5.1 and appendix D we will discuss, instead, procedures that lead to discoveries at multiple resolutions, in a coordinated fashion.

We also want to underscore how the notion of resolution-adaptive discovery is relevant also for families of hypotheses that are not associated to spatial localization of a signal. For example, as in [Cortes et al. \(2017\)](#), low resolution hypotheses might correspond to group of traits, and the precision of discoveries increases as more specific statements can be made about which traits are involved. We will consider related problems in sections 5.3 and 6.3.

Finally, note that it is also possible to generalize the above definition of \mathcal{A}^1 to sets containing multiple “individual” hypotheses, as long as these are always tested together.

3 eLP: an e-value based linear program for controlled, resolution-adaptive discoveries

We now describe a multiple testing procedure that achieves the goal in (3)-(5). The procedure evaluates the evidence in favor of the hypotheses in \mathcal{H} by using e-values. The term e-value has been introduced recently and encompasses multiple related alternative approaches to testing, including betting scores and likelihood ratios ([Vovk and Wang, 2021](#); [Shafer, 2021](#); [Grünwald et al., 2020](#)). Like p-values, e-values are defined by their properties under the null hypothesis; however, while p-values are defined in terms of probabilities, e-values are defined in terms of expectations. Formally, a p-value P is a random variable that satisfies $\mathbb{P}_{null}(P \leq \alpha) \leq \alpha$ (often with equality) for all $\alpha \in (0, 1)$. In other words, a p-variable is stochastically larger than $U[0, 1]$ under the null. An e-value E is a $[0, \infty]$ -valued random

variable satisfying $\mathbb{E}_{null}[E] \leq 1$. We can conceptualize it as the stochastic return of a bet against the null hypothesis: on average, if the null is true, it multiplies the money risked by 1 (no gain), and large gains are unlikely (by Markov’s inequality a gain larger than a constant c happens with probability at most $1/c$). A large realized e-value, a substantial win in the bet, indicates that the null is unlikely to be true so that the e-value can be interpreted as the amount of evidence collected against the null. Indeed, it has been argued that, for the general public, a summary of evidence given in terms of return on a bet might be easier to interpret than the p-value (Shafer, 2021).

Aside from this possible increased efficacy in communication, the fact that e-values are defined in terms of expectation translates in a number of advantages from the point of view of designing valid (multiple) testing strategies (Wang and Ramdas, 2022). For example, in contrast to p-values, handling dependent e-values is quite straightforward due to the linearity of expectation. Crucially for our purposes, to establish that a multiple testing procedure controls FDR when it is based on e-values with any dependence structure, it is sufficient to verify that it is self-consistent. This is a purely algorithmic property, originally introduced in Blanchard and Roquain (2008) with reference to p-values. Wang and Ramdas (2022) translate it to the e-value context. Let $e_1, \dots, e_{|\mathcal{H}|}$ be e-values associated with hypotheses $H \in \mathcal{H}$. They define an e-testing procedure \mathcal{F} to be self-consistent at level $\alpha \in (0, 1)$ if, for every rejected hypothesis H_k , the corresponding e-value e_k satisfies

$$e_k \geq \frac{|\mathcal{H}|}{\alpha R_{\mathcal{F}}}, \quad (6)$$

where $|\mathcal{H}|$ denotes the total number of hypotheses and $R_{\mathcal{F}}$ denotes the number of rejections. Wang and Ramdas (2022) show that self-consistency is a sufficient condition for FDR control, with arbitrary configurations of e-values. This is in contrast to what happens for p-values, where an additional dependency control condition is needed (Blanchard and Roquain, 2008). Note that the numerator of equation (6) depends on the number of hypotheses tested, which can make relying on self-consistency for frequentist FDR control conservative.

Similarly to Spector and Janson (2023), we can then define a linear program that achieves the goal in (3)-(5).

Procedure 1. eLP, e-value linear programming. *Let \mathcal{H} be a multi-resolution family of hypotheses, corresponding to a collection of groups \mathcal{A} , defined starting from p individual hypotheses. Let each hypothesis be associated with an e-value e_A and a weight $w(A)$ for $A \in \mathcal{A}$. Let $\alpha \in (0, 1)$ be the desired level of FDR control and let $x_A \in \{0, 1\}$ be an indicator of whether the hypothesis H_A is rejected. The rejection set of eLP is identified by solving the following*

constrained optimization:

$$\max_{\{x_A\}_{A \in \mathcal{A}}} \sum_{A \in \mathcal{A}} w(A)x_A \quad (7a)$$

$$\text{subject to } x_A \in \{0, 1\} \quad \forall A \in \mathcal{A} \quad (7b)$$

$$|\mathcal{A}| - \alpha e_A \sum_{A \in \mathcal{A}} x_A \leq |\mathcal{A}| \times (1 - x_A) \quad \forall A \in \mathcal{A}, \quad (7c)$$

$$\sum_{A \in \mathcal{A}: j \in A} x_A \leq 1 \quad \forall j \in \{1, \dots, p\}. \quad (7d)$$

The first constraint (7b) simply characterizes $x_A \in \{0, 1\}$ as an indicator. The objective (7a) corresponds to our goal in (3). The linear constraint (7c) ensures frequentist FDR control at level α . The sum $\sum_{A \in \mathcal{A}} x_A$ equals the number of rejections by the procedure. Then, if $x_A = 1$, (7c) requires that $e_A \geq \frac{|\mathcal{A}|}{\alpha \sum_{A \in \mathcal{A}} x_A}$, which is exactly the self-consistency condition in equation (6). If $x_A = 0$, (7c) is automatically satisfied, as $\alpha e_A \sum_{A \in \mathcal{A}} x_A \geq 0$. Constraint (7d) ensures that the rejected regions are disjoint (5): each $j \in \{1, \dots, p\}$ can be rejected at most once, and not multiple times in different groups.

Remark 1 To use eLP, researchers need to have available e-values for all the hypotheses. In case the testing procedure leads to p-values, it is possible to convert these to e-values using “calibration,” albeit with possible power loss (see [Vovk and Wang \(2021\)](#)).

Remark 2 A consequence of the linearity of expectation is that an arithmetic mean of e-values of individual hypotheses belonging to a certain group is an e-value for their group-level global null hypothesis. In fact, the arithmetic mean essentially dominates any symmetric e-merging function, i.e. functions that take e-values of individual hypotheses as input and provide an e-value for the group-level global null as output (see [\(Vovk and Wang, 2021\)](#), who also discuss cross-merging functions, mapping several p-values into an e-value). Note that if group e-values are constructed with this strategy, eLP would only reject hypotheses at the finest level of resolution (the individual level). We describe how to get non-trivial group e-values from the knockoff filter in section 4.

Remark 3 For a single level of resolution, that is $|\mathcal{M}| = 1$, eLP reduces to the e-BH procedure by [Wang and Ramdas \(2022\)](#).

Self-consistency can also be used to define other multiple comparisons procedures based on e-values. For example, as mentioned in [Wang and Ramdas \(2022\)](#), one can construct the equivalence of Focused BH ([Katsevich et al., 2021](#)) for e-values. We do so precisely in appendix B, obtaining a procedure we call Focused e-BH and which controls FDR for any filter and under any dependence structure.

Focused e-BH applied to a multi-resolution family of hypotheses with a filter that selects the most precise non-redundant rejections produces the same rejection set of eLP with weights

$w(A) = 1/|A|$; see appendix B for more details. This is interesting in the context of the comparison in Spector and Janson (2023) between Focused BH and BLiP, which showed larger power for BLiP. This equivalence relationship between eLP (which has many commonalities with BLiP) and Focused e-BH (which is a translation of Focused BH to e-values) underscores how—when considering exactly the same set of hypotheses—the observed difference in power might not be due to the linear programming formulation, but rather to the implicit estimate of the FDR underlying these two methods. Spector and Janson (2023) control the Bayesian FDR, which can be evaluated using posterior probabilities. Focused BH and Focused e-BH control the frequentist FDR. A (self-consistent) procedure controlling the frequentist FDR bounds the number of wrong rejections utilizing the total number of hypotheses tested: this can lead to conservative behavior, when non-redundancy constraints limit the number of possible rejections to a value much smaller than the total count of tested hypotheses. To remedy this, Katsevich et al. (2021) introduced a permutation based method to estimate the number of false rejections, which, however, comes with computational costs.

4 KeLP: eLP with knockoff e-values

Given e-values for a family of hypotheses \mathcal{H} , eLP guarantees FDR control while leading to resolution-adaptive discoveries. However, defining powerful e-values is a non-trivial task (Vovk and Wang, 2021). We now describe how to accomplish this for specific types of multi-resolution families of hypotheses leveraging the knockoff framework (Barber and Candès, 2015; Candès et al., 2018).

For a set of p explanatory variables $X = (X_1, \dots, X_p)$ and a response Y , the knockoff framework tests, with FDR control, conditional independence hypotheses

$$H_j : Y \perp\!\!\!\perp X_j \mid X_{-j} \quad (8)$$

and, given a partition \mathcal{A}^m , their group equivalent

$$H_{A_g^m} : Y \perp\!\!\!\perp X_{A_g^m} \mid X_{-A_g^m} \quad (9)$$

where $X_{A_g^m} = \{X_j\}_{j \in A_g^m}$ and $X_{-A_g^m}$ denotes all features except X_j with $j \in A_g^m$ (Katsevich and Sabatti, 2019; Sesia et al., 2020).

The knockoff framework relies on two steps: a) the construction of test statistics with some distributional properties under the null and b) a multiple comparison procedure. The first step a) is based on comparing the signal of each feature (or group of features) with that of a “knockoff copy” of it, indistinguishable from the original in distribution, but independent from Y (Candès et al., 2018; Sesia et al., 2020). This is done with a score W_j designed so that swapping the original feature X_j with its knockoff \tilde{X}_j flips the sign of W_j . For example, a popular choice (Candès et al., 2018) for the scores is the difference of the absolute values

of the coefficients based on a cross validated Lasso of Y on the entire collection of original features and knockoffs: $W_j = |\beta_j| - |\tilde{\beta}_j|$, where β_j is the resulting coefficient of X_j and $\tilde{\beta}_j$ the coefficient of the knockoff \tilde{X}_j . A large value of W_j suggests greater evidence against the null.

The b) multiple comparison procedure (filter) is based on an estimate of the FDP that relies on the distribution of the knockoff scores W_j corresponding to null hypotheses. Precisely, to control FDR at level γ , the knockoff filter (Barber and Candès, 2015) selects the set of features \mathcal{R}_{KO} according to the following rule:

$$\begin{aligned}\mathcal{R}_{\text{KO}} &= \{j : W_j \geq T\} \\ T &= \inf\{t > 0 : \frac{1 + \sum_{j \in [p]} \mathbf{1}\{W_j \leq -t\}}{\sum_{j \in [p]} \mathbf{1}\{W_j \geq t\}} \leq \gamma\}.\end{aligned}\tag{10}$$

The martingale properties that guarantee that (10) controls FDR at level γ also guarantee that:

$$\mathbb{E}\left[\frac{\sum_{j: H_j \in \mathcal{H}_0} \mathbf{1}\{W_j \geq T\}}{1 + \sum_{j: H_j \in \mathcal{H}_0} \mathbf{1}\{W_j \leq -T\}}\right] \leq 1.\tag{11}$$

This expectation motivated the construction in Ren and Barber (2023), who show how the rejections of the knockoff filter are equivalent to those of e-BH applied to e-values defined as

$$e_j := p \cdot \frac{\mathbf{1}\{W_j \geq T\}}{1 + \sum_{k \in [p]} \mathbf{1}\{W_k \leq -T\}}.$$

Note that these e_j are not strictly e-values: it is not true that for each null $\mathbb{E}[e_j] \leq 1$, but only that $\sum_{j: H_j \in \mathcal{H}_0} \mathbb{E}[e_j] \leq p$. This property follows from equation (11), as

$$\sum_{j: H_j \in \mathcal{H}_0} \mathbb{E}[e_j] = p \cdot \sum_{j: H_j \in \mathcal{H}_0} \mathbb{E}\left[\frac{\mathbf{1}\{W_j \geq T\}}{1 + \sum_{k \in [p]} \mathbf{1}\{W_k \leq -T\}}\right] \leq p \cdot \mathbb{E}\left[\frac{\sum_{j: H_j \in \mathcal{H}_0} \mathbf{1}\{W_j \geq T\}}{1 + \sum_{j: H_j \in \mathcal{H}_0} \mathbf{1}\{W_j \leq -T\}}\right] \leq p.$$

Nevertheless, Ren and Barber (2023) show that this property of “relaxed” e-values is sufficient to guarantee FDR control in the rejections defined with e-BH.

Describing the knockoff filter in terms of e-BH applied to e-values is convenient because of the advantages of this framework in dealing with dependency. Ren and Barber (2023) show, for example, how dependent sets of $\{e_j^k, j = 1, \dots, p\}$, derived from k runs of the knockoff procedure, can be combined to achieve a stable variable selection. This is also useful in our multi-resolution framework. To illustrate this, we start generalizing the result by Wang and Ramdas (2022) for relaxed e-values.

Theorem 1. *Suppose $\mathbf{e} = (e_1, \dots, e_n)$ are relaxed e-values for hypotheses (H_1, \dots, H_n) , i.e. they satisfy $\sum_{j: H_j \in \mathcal{H}_0} \mathbb{E}[e_j] \leq n$. Then any self-consistent e-testing procedure \mathcal{F} at level α taking \mathbf{e} as input controls the FDR at level α .*

The proof is almost identical to the proof in Wang and Ramdas (2022) and is included in appendix A. Theorem 1 guarantees that we can use relaxed e-values as an input to eLP (Procedure 1). The following describes the construction of knockoffs-based e-values for the hypotheses at each resolution and their use in a procedure we call KeLP. \tilde{X}^m is said to be a (group) knockoff for partition $m \in \mathcal{M}$ if for each group $A_g^m \in \mathcal{A}^m$ it holds that $(X, \tilde{X}^m)_{\text{swap}(A_g^m, \mathcal{A}^m)} \stackrel{d}{=} (X, \tilde{X}^m)$ and Y is independent of \tilde{X}^m given X ; see e.g. Sesia et al. (2021). $(X, \tilde{X}^m)_{(\text{swap}_{A_g^m}, \mathcal{A}^m)}$ means that the j -th coordinate is swapped with the $(j+p)$ -th coordinate for all $j \in A_g^m$. The construction of (group) knockoff variables has been studied in prior research; see for example Sesia et al. (2019, 2021); Dai and Barber (2016); Katsevich and Sabatti (2019); Gimenez et al. (2019); Spector and Janson (2022); Romano et al. (2020).

Procedure 2. (KeLP, knockoff e-value linear programming) Let \mathcal{H} be a multi-resolution family of conditional independence hypotheses relative to variables Y, X_1, \dots, X_p . For each resolution $m \in \mathcal{M}$, construct (group) knockoffs for X_1, \dots, X_p with respect to partition \mathcal{A}^m and obtain for each hypothesis $H_{A_g^m}$ the knockoff score $W_{A_g^m}$. Let $\{c_m\}_{m \in \mathcal{M}}$ be non-negative numbers such that $\sum_{m \in \mathcal{M}} c_m \leq |\mathcal{A}|$. For each $m \in \mathcal{M}$, define knockoffs-based e-values by

$$e_{A_g^m} := c_m \cdot \frac{\mathbf{1}\{W_{A_g^m} \geq T^m\}}{1 + \sum_{A \in \mathcal{A}^m} \mathbf{1}\{W_A \leq -T^m\}}, \quad \text{where} \quad (12)$$

$$T^m = \inf\{t > 0 : \frac{1 + \sum_{A \in \mathcal{A}^m} \mathbf{1}\{W_A \leq -t\}}{\sum_{A \in \mathcal{A}^m} \mathbf{1}\{W_A \geq t\}} \leq \gamma^m\}, \quad \gamma^m \in (0, 1). \quad (13)$$

For a fixed weighting function $w(\cdot)$ and a target FDR level α , the rejection set of KeLP is given by the output of eLP (Procedure 1) taking these and the e-values (12) as input.

Due to the correspondence between the e-BH procedure by Wang and Ramdas (2022) and the traditional knockoff-filter by Candès et al. (2018), as described by Ren and Barber (2023), if $|\mathcal{M}| = 1$, KeLP is equivalent to the usual knockoff procedure.

There are two sets of parameters in KeLP: c_m and γ^m . In (12), c_m is a fixed multiplier that is chosen to guarantee the property for theorem 1:

$$\sum_{A: H_A \in \mathcal{H}_0} \mathbb{E}[e_A] = \sum_{m \in \mathcal{M}} \sum_{A_g^m: H_g^m \in \mathcal{H}_0^m} \mathbb{E}[e_{A_g^m}] \leq \sum_{m \in \mathcal{M}} c_m \leq |\mathcal{A}|. \quad (14)$$

The first inequality follows from the property of the importance statistics in equation (11), and the second is true by construction (note that it is possible for some $c_m > |\mathcal{A}^m|$, which relaxes the original definition of knockoff-based e-values by Ren and Barber (2023), since for our goal in (3)-(5) we are not going to apply e-BH to each resolution separately).

The parameter γ^m used to obtain the stopping time T^m (13) governs the trade-off between the number of non-zero e-values and their magnitude. For a larger γ^m , we might obtain

a smaller T^m , which might result in a larger number of non-zero e-values. However, those nonzero e-values might be smaller in magnitude, as there might also be more groups with $W_{A_g^m} \leq -T^m$.

The choice of c_m and γ^m is left to the user, and can be guided by tuning in a hold-out dataset. However, note that even in a GWAS setting a “large” tuning set might not be required; see appendix F for details. In this work, we set $c_m = |\mathcal{A}|/|\mathcal{M}|$. This choice results in knockoff e-values whose magnitude depends mostly on signal-strength, and not on the number of groups in a particular resolution. KeLP already includes the preference to reject hypotheses in smaller levels of resolution. As for γ^m , in applications with moderate dimensions, following Ren and Barber (2023), we recommend $\gamma^m = \alpha/2$ or $\gamma^m = \alpha/4$, where $\gamma = \alpha/4$ should be chosen in higher dimensional settings. We suggest level-specific choices of γ^m for very high-dimensional applications with many levels of resolution and very sparse signals (e.g. genetic data): in this case, we recommend choosing $\gamma = \alpha$ for the individual level, with decreasing levels of γ as the resolutions becomes coarser. We leave the question of finding the optimal theoretical parameters for further research. We solve the linear program corresponding to KeLP using a standard optimization software: CVXR (Fu et al., 2020).

5 Additional applications of knockoff e-values and KeLP

Before exploring the performance of KeLP with simulations and real-data analysis, we pause to illustrate other advantages of e-values and of re-casting knockoff analyses in this framework (12). We consider two cases in which the dependency between p-value/test statistics presented challenges for analysis, and underscore the generality of KeLP by showing how it can be leveraged to analyze multivariate structured outcomes.

5.1 Multilayer Knockoff Filter

As mentioned in section 2, when working with hypotheses at multiple resolutions, different notions of global error are meaningful. The goal of this paper is to reject the most specific hypotheses possible, while controlling the FDR across the rejection set, which might span multiple levels of resolution.

Another goal, referred to as multilayer FDR control, is to coordinate rejections across resolutions and provide simultaneous FDR control in each resolution. Barber and Ramdas (2017) introduced multilayer FDR control and developed the p-filter, which attains it when the p-values for the individual hypotheses are PRDS and group hypotheses are tested using Simes’s combination rule (Simes, 1986).

The original p-filter by Barber and Ramdas (2017) has been extended to arbitrary dependencies between the p-values in Ramdas et al. (2019b) using reshaping, which makes the procedure conservative.

E-values can be used to develop an analog of the p-filter, as mentioned by [Wang and Ramdas \(2022\)](#). We include a description of the e-filter in appendix [D](#).

[Katsevich and Sabatti \(2019\)](#) developed the Multilayer Knockoff Filter (MKF) to attain the same goal in the context of a multi-resolution analysis via knockoffs. The MKF controls the FDR at level $\alpha \times \kappa$, where $\kappa \approx 1.93$ and α denotes the target FDR level. Using knockoff e-values, we describe the e-Multilayer Knockoff Filter (e-MKF) with FDR control at the target level α in appendix [D](#). We also show that, for the same theoretical level of FDR control, the e-MKF has higher power compared to the MKF.

5.2 Partial conjunction hypotheses

A multi-resolution family of hypotheses is one type of “structured” collection of hypotheses. Another type that is often useful to consider is the one motivating partial conjunction testing ([Benjamini and Heller, 2008](#)). Here one can think about an array of hypotheses $\{H_j^\ell\}_{j=1, \ell=1}^{n, L}$, where for each j , researchers are interested to discover that at least u out of L tested hypotheses are false. One context where partial conjunctions are quite relevant is replication ([Bogomolov and Heller, 2013, 2018](#)). For example, the genetic underpinnings of a disorder might be studied in different human populations, and scientists might be interested in identifying those SNPs that carry a signal in at least u distinct groups. A related, but different, example, in the context of GWAS, is when measurements on several phenotypes may be available. Scientists might then be interested in testing whether a SNP (or group of SNPs) is conditionally independent of *any* (or *at least* a certain number) of the phenotypes.

[Li et al. \(2022\)](#) developed a knockoff filter to test partial conjunctions across distinct independent studies. This approach, however, cannot be applied to the investigation of multiple phenotypes collected on the same individuals—the knockoff scores relative to the different phenotypes being based on the same genotype data are going to be dependent. Using knockoff e-values we can overcome this limitation, as we describe in the appendix [C](#). Testing these partial conjunction hypotheses can also be combined with testing across multiple levels of resolution. Indeed, in our application to the UK Biobank data in section [7](#), we test a global null hypothesis for platelet-related outcomes.

5.3 Structured outcomes

In some cases, it might be possible to describe a hierarchy among the outcomes ([Cortes et al., 2017](#)). Let L denote the total number of outcomes. To fix ideas, consider the example in [Figure 3](#). The binary tree has four leaves, two internal nodes and one root node. Each of the parent nodes is constructed as a union of its leaf descendants.

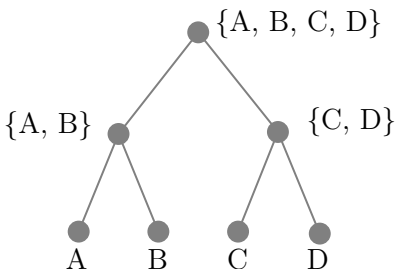


Figure 3: Illustration of an outcome structure corresponding to a binary tree with seven nodes based on four leaves A, B, C and D . Each parent node is constructed based on its children.

We are interested in testing conditional independence hypotheses between each of the p features and the $L = 7$ different outcomes. Even without considering different groupings of the p features, there is a level of redundancy between the hypotheses. For example, rejecting the hypotheses of conditional independence between feature X_j and both $\{A, B\}$ and A is redundant, as it implicates the leaf-outcome A twice and stating that X_j is not independent from A logically implies that X_j is not independent from $\{A, B\}$.

We can use the KeLP framework to filter rejections so that they point to the most specific outcome for each feature. Specifically, we obtain one knockoff e-value for each feature for each node of the tree shown in Figure 3, i.e. seven knockoff e-values for each feature in total. We require that the hypothesis of conditional independence from each feature be rejected only once for each leaf-outcome. We weigh hypotheses with the reciprocal of the number of leaf-outcomes they implicate. With these specifications, we can then apply KeLP to the $7 \times p$ e-values in total, controlling the FDR across the entire rejected set (across all outcomes and features).

The output of the procedure returns separately for each feature the most specific outcome for which the conditional independence hypothesis was rejected. We show a simulation of this setting in section 6.3.

6 Simulations

To illustrate KeLP’s power in localizing signals among features we use two simulation settings: in the first, the features are generated with a block-diagonal variance covariance matrix and in the second they are genotypes of SNPs on chromosome 21 of the White Non-British population of the UK Biobank. We also explore KeLP’s performance with structured outcomes, as in Figure 3. The code for the simulations is available at: <https://github.com/pmgblz/KeLP>.

6.1 Block-diagonal correlation structure for features

We simulate n observations of the outcome from $Y | X \sim N(X^T \beta, I_n)$, with I_n the identity matrix. The feature vector $X \in \mathbb{R}^p$ is generated as $X \sim N(0, \Sigma)$, where Σ is block-diagonal with blocks of size 5 and $p = 1,000$. Within each block, the correlation pattern follows an AR(1) process with $\Sigma_{jk} = 0.8^{|j-k|}$. This provides a schematic representation of the dependence structure between DNA polymorphisms. Following further [Spector and Janson \(2023\)](#), there are $s \times p$ randomly chosen nonzero coefficients, rounded to the nearest integer, where $s \in (0, 1)$ denotes the sparsity. The nonzero coefficients are simulated as i.i.d. $N(0, \tau^2)$ with $\tau = 0.2$. Across the simulations, we vary the ratio n/p , starting at $n/p = 0.1$.

We consider two levels of resolutions: the individual level (groups of size 1) and groups of size 5. The (group) knockoff variables are generated following the maximum entropy criteria ([Spector and Janson, 2022](#); [Chu, 2023](#)); see appendix E for details.

We compare KeLP’s rejection sets with those of the knockoff filter applied separately at each level of resolution (“Knockoffs individual” and “Knockoffs group”), as well as two other approaches to identify rejections across resolutions. The first (“Knockoffs outer”) consists in simply identifying the outer-nodes of the rejections that the knockoff filter makes at each resolution. Outer-nodes are those groups of variables with no rejected descendants, where a descendant is a group contained within the parent group (see Figure 1). Note that filtering the resolution-specific rejections by the knockoff filter to the outer-nodes does not have guarantees on FDR control. To obtain FDR control at level α on the filtered outer-nodes, it is possible to run e-BH on their corresponding knockoff e-values at the amended level $\tilde{\alpha} = \alpha |S| / |\mathcal{H}|$, where $|S|$ denotes the number of filtered outer-nodes. This ensures self-consistency; see [Wang and Ramdas \(2022\)](#). We include this procedure (“e-BH knockoffs outer”) in our comparisons.

To evaluate performance, we look at FDP, power and precision of discoveries. The realized FDP is calculated separately for each level of resolution for the knockoff filter (individual and group) and across the resolutions for the other methods. We define “power” as the number of correctly rejected nonzero individual features (whether they were rejected individually or in a group), divided by the total number of nonzero individual features. To evaluate the precision of discoveries we look at the total number of features included in the rejected groups. For a given level of power, the most precise method points to the smallest number of features.

Figure 4 shows that the methods perform as expected in terms of FDR control. In terms of power and size of the rejection set, KeLP effectively “interpolates” between the individual and the group level. For lower levels of signal strength, KeLP rejects more groups than individual features, but achieves the precision of the individual level as signal strength increases. KeLP’s power is very close to that of the outer-nodes of the knockoff filter applied separately at each resolution, but achieves FDR control. Refining the outer-nodes with e-BH leads to no power.

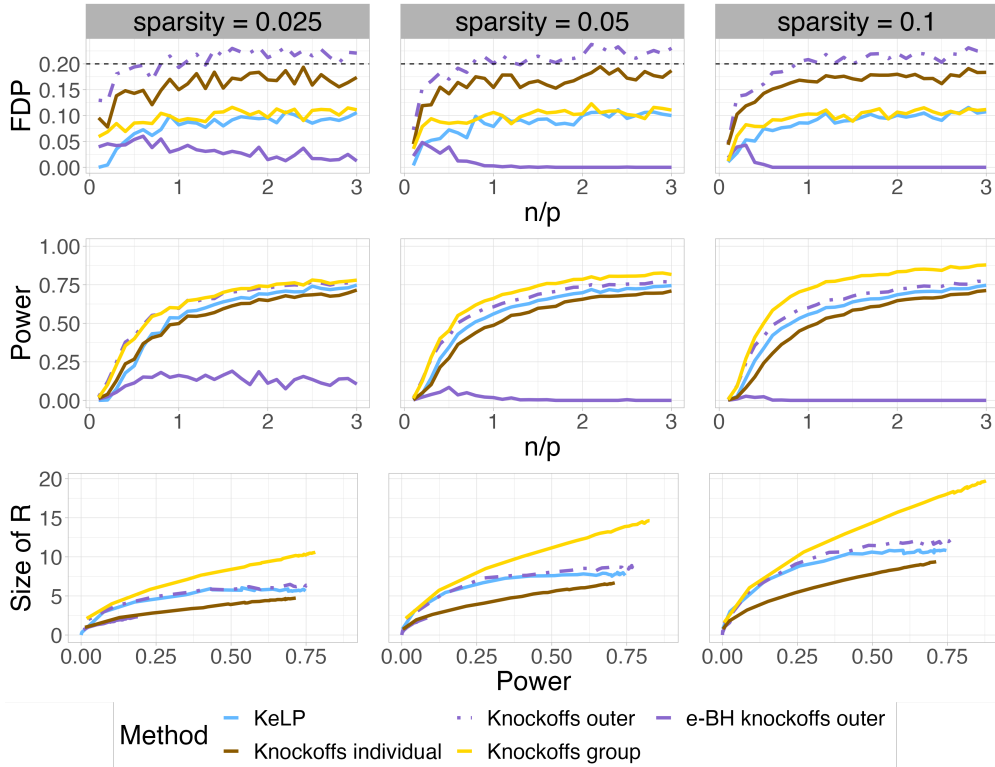


Figure 4: By row, FDP, power, and size of the rejection set, averaged across 100 simulation runs. By columns, different signal sparsities (corresponding signal to noise ratios are 1, 2 and 4, from left to right). Target FDR is indicated with a dashed line. The size of the rejection set is displayed as the square root of the total number of variables included in the rejected hypotheses. Broken lines are used for methodologies not expected to control FDR. Colors in the blue-purple spectrum indicate procedures whose rejection sets span across multiple resolutions.

6.2 Chromosome-wide simulation on the UK Biobank genotypes

We again simulate $Y | X \sim N(X^T \beta, I_n)$. Here, X are the genotypes of chromosome 21 of the unrelated White Non-British population of the UK Biobank with $p = 8,832$ and $n = 14,733$. We use the ancestries, resolutions and knockoffs defined by [Sesia et al. \(2021\)](#); see also appendix F for more details. We compare the same methods as in section 6.1. There are $s \times p$ randomly chosen nonzero coefficients across chromosome 21, rounded to the nearest integer. As n and p are fixed in this setting, to explore different signal strengths, we vary the absolute value of the nonzero elements β : these are set to a/\sqrt{n} , where a denotes the signal amplitude. The signs of the nonzero coefficients are determined by independent coin

flips.

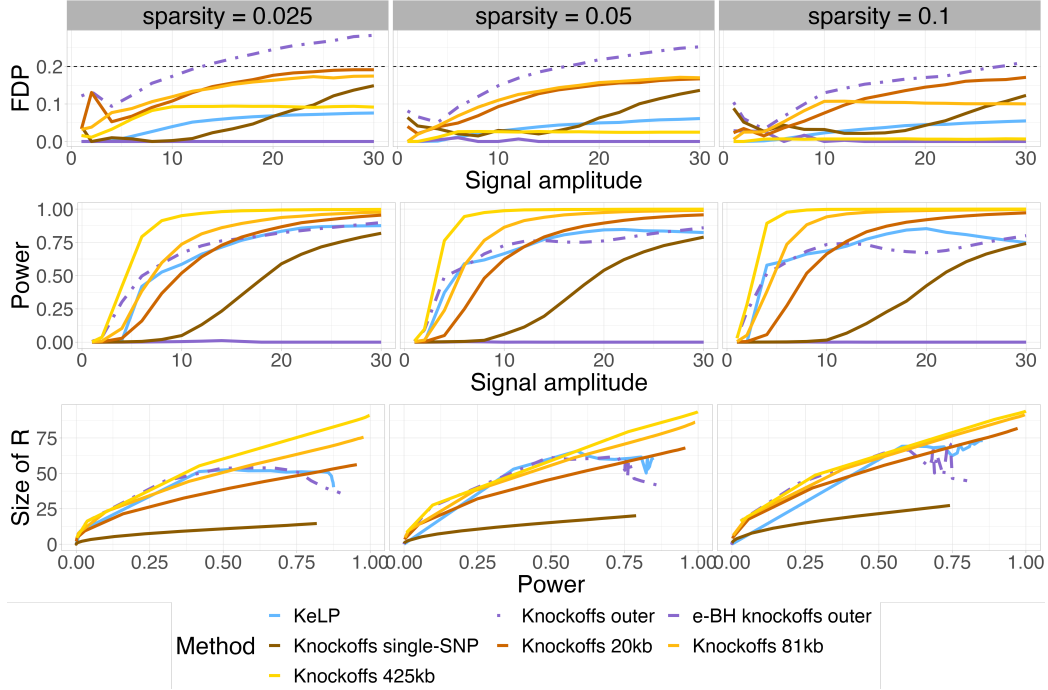


Figure 5: By row, FDP, power, and size of the rejection set, averaged across 25 simulation runs. By columns, different signal sparsities. Figure 9 in appendix E shows heritability ($\text{Var}(f(X))/\text{Var}(Y) = \text{Var}(X\beta)/\text{Var}(X\beta + \epsilon)$) as a function of signal amplitude. See caption of Figure 4 for details. Resolutions are indicated by median group width in kilobases (kb); see Sesia et al. (2021) for further details.

Figure 5 shows similar results to those in Figure 4: KeLP leads to a rejection set comparable to that of knockoffs outer-nodes, while controlling the FDR at the desired level.

6.3 Structured outcomes

We consider outcomes with a structure that corresponds to the tree in Figure 3. In particular, consider a setting where the outcomes corresponding to leaves refer to the most specific diseases. We denote by cases the proportion of people who have these diseases. Let $\ell \in \{1, \dots, L\}$ with $L = 7$ indicate the node. Each of the four leaves is simulated from a logistic model $Y_\ell | X \sim \text{Bernoulli}((1 + e^{-(\delta_\ell + X^T \beta_\ell)})^{-1})$ where δ_ℓ is an intercept chosen to obtain an approximate percentage of cases of 15% for each of the leaves. We simulate $X \in \mathbb{R}^p$ as $X \sim N(0, \Sigma)$, where Σ has entries $\Sigma_{jk} = 0.3^{|j-k|}$ and $p = 1,000$. There are $s \times p$

randomly chosen nonzero coefficients, rounded to the nearest integer, where $s \in (0, 1)$ denotes the sparsity. We also set an overlap of 50% for the nonzero features between each of the siblings corresponding to the same internal parent node. The magnitudes of the nonzero coefficients are simulated as i.i.d. $N(\mu, \tau^2)$ with $\mu = 1$ and $\tau = 0.5$. We define the binary outcomes corresponding to the parent nodes in the tree to be equal to 1 whenever any of their descendants is equal to 1. Across the simulations, we vary the ratio n/p , starting at $n/p = 0.1$.

In this hierarchical setting, it makes sense to consider the properties of rejection sets at each level of the tree, or among outer-nodes. We compare the performance of KeLP, the combined results of the knockoff filter for the outcomes at each level of the tree (“knockoffs leaves”, “knockoffs internal nodes”, “knockoffs root node”) and the corresponding outer-nodes.

The knockoff filter for the outcome corresponding to the root node has FDR control. However, the rejection set obtained by combining the results of the knockoff filter run separately for the two outcomes corresponding to internal nodes does not have FDR control (as we are simultaneously considering multiple outcomes). Neither does the rejection set that collects all discoveries made by the knockoff filter separately run on the leaf-outcomes. As before, to obtain FDR control, we pass these through a further e-BH procedure at the amended level $\tilde{\alpha} = \alpha|S|/|\mathcal{H}|$ (“e-BH knockoffs leaves”, “e-BH knockoffs internal”), where $|S|$ denotes the number of rejections by the knockoff filter collected across multiple outcomes, but within the same level of the tree, and $|\mathcal{H}|$ the total number of hypotheses at the specific level of the tree.

Consider the tree in Figure 3: each leaf-outcome is associated with a set of nonzero features. We call the sum of the number of nonzero features across the leaf-outcomes the “total number of nonzero leaf-outcome associations”. Moreover, if, for example, feature X_j is nonzero for outcome A , it is also nonzero for the outcome corresponding to the internal node $\{A, B\}$ and the root node $\{A, B, C, D\}$. Therefore, if X_j is rejected at the level of the internal node or the root node, it is also counted as a correct rejection. We then define power as the total number of correct rejections divided by the total number of nonzero feature-outcome associations. We calculate power and FDR separately at each level of the tree for the rejection set obtained by combining the results of the knockoff filter at each level and across levels for KeLP and the knockoffs outer-nodes.

The discovery of an association between X_j and both $\{A\}$ and $\{B\}$ is more precise than the discovery of an association between X_j and $\{A, B\}$. In agreement with the weighting scheme we described in section 5.3, we measure precision in terms of number of “individually” associated outcomes. The rejection of the hypothesis of conditional independence between X_j and each of the leaves A, B, C, D adds 1 to this count; the rejection of an internal node adds 1/2, and the rejection of the root node adds 1/4.

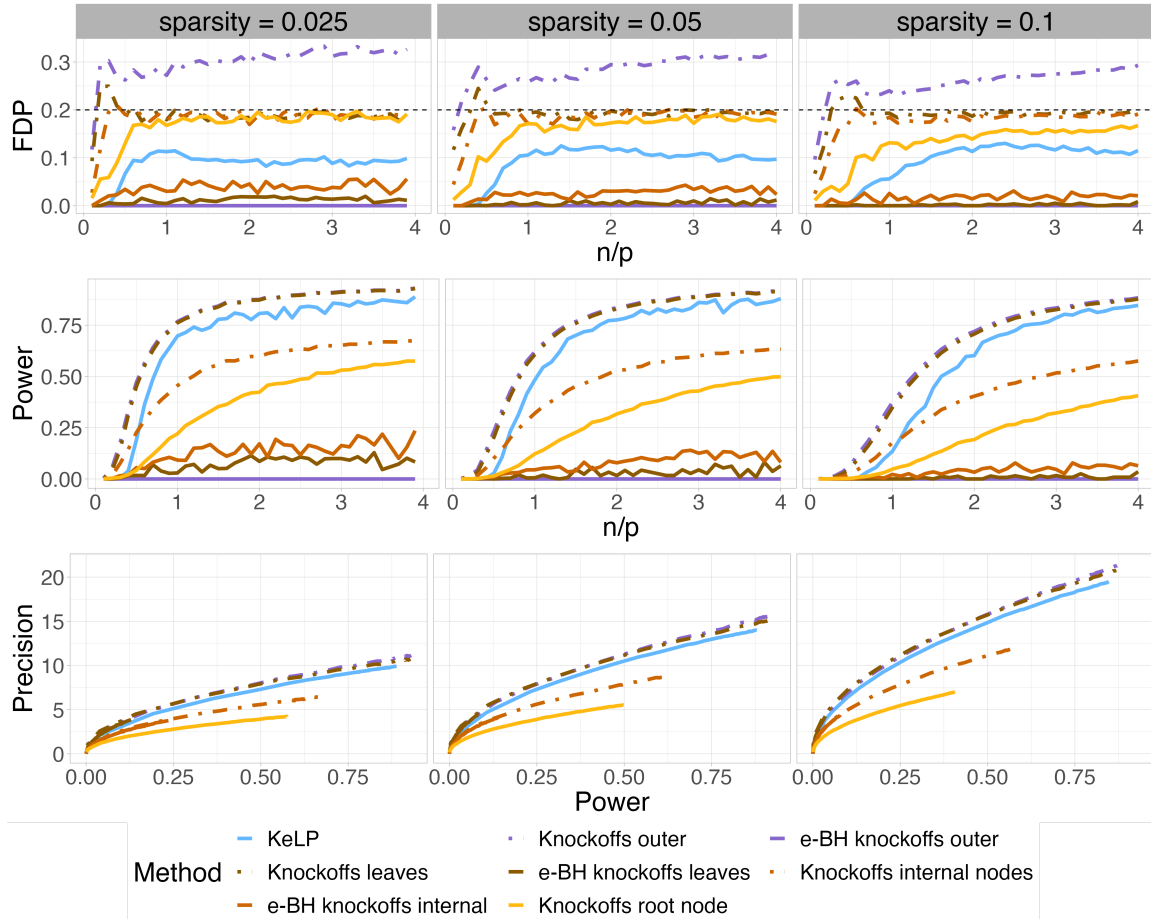


Figure 6: By row, FDP, power, and the square root of the number of singularly implicated outcomes (“precision”), averaged across 100 simulation runs. By columns, different signal sparsities. Target FDR is indicated with a dashed line. Broken lines are used for methodologies not expected to control FDR. Colors in the blue-purple spectrum indicate procedures whose rejection sets span across multiple levels of the tree. Note that, unlike in Figures 4 and 5, higher values are preferred in the bottom panel. The power and precision curves for “Knockoffs outer” and “Knockoffs leaves” almost coincide.

Figure 6 shows that KeLP has FDR control, as expected from the theoretical results in section 4. Moreover, in terms of power and precision, it behaves similarly to the knockoffs outer-nodes. However, the knockoffs outer-nodes violate FDR control. Moreover, KeLP has highest power among all methods with theoretical FDR control (all solid lines in Figure 6).

7 Application to the UK Biobank

We use KeLP to analyze the relation between two phenotypes (height and platelets) and genetic variation in approximately 337k British unrelated individuals of the UK Biobank. The genotype data consists of about 592k autosomal SNPs. We consider seven different partitions of SNPs corresponding to different resolutions, as in [Sesia et al. \(2021\)](#) and rely on the knockoffs generated in that study to construct e-values (12) for all group hypotheses. Our target FDR level is $\alpha = 0.1$.

Table 1 shows, stratified by resolution, the number of rejections and of implicated SNPs by (1) KeLP, (2) the knockoff filter applied to each resolution separately, and (3) the outer-nodes of the knockoffs rejections. Appendix F.1.1 provides a visualization of the KeLP rejection regions.

Table 1: UK Biobank: height

Resolution	Number of rejections			SNPs implicated		
	KeLP	Outer-nodes	Res. spec.	KeLP	Outer-nodes	Res. spec.
single-SNP	53	53	53	53	53	53
3 kb	148	260	313	1,545	2,549	3,010
20 kb	245	932	1,215	6,587	20,455	26,909
41 kb	345	1,024	2,139	12,079	31,480	68,070
81 kb	711	891	2,817	34,715	38,732	132,493
208 kb	555	882	3,159	47,387	65,595	267,712
425 kb	406	371	2,783	55,338	44,431	396,238
Total	2,463	4,413		157,704	203,295	

British unrelated population. FDR level: $\alpha = 0.1$. The column “Res. spec.” (resolution specific) reports the results of the knockoff filter applied separately at each level of resolution (these rejection sets have FDR control at the resolution level, but are redundant across resolutions). The column “Outer-nodes” refers to the results of filtering these resolution-specific knockoffs rejections (which leads to a rejection set with no FDR control). Resolutions are indicated by median group width in kilobases (kb); see [Sesia et al. \(2021\)](#) for further details.

To explore the validity of the KeLP rejections, we compare them to the discoveries in [Yengo et al. \(2022\)](#), who find 12,111 independent SNPs that are significantly associated with height on the basis of a COJO (conditional and joint association analysis with summary statistics) analysis based on GWAS data of 5.4 million individuals. For this analysis, we consider groups which do not contain any of these SNPs (matching by name or location) as true nulls, and evaluate their discoveries as false. The derived estimate of FDP for KeLP is around 7.5%, while that of the knockoffs outer-nodes is approximately 20%—substantially higher than the target FDR level of 10%. The rejections by KeLP include 4,121 SNPs out of the 12,111 SNPs in [Yengo et al. \(2022\)](#), while 5,203 of these are discovered by the knockoffs outer-nodes: the increased FDP of this last approach comes with low power rewards.

We consider four continuous platelet-related phenotypes (platelet count, platelet crit, platelet width, platelet volume) and look for locations in the genome associated to any of them. To

obtain global null e-values for each group at each level of resolution, we average the knockoff e-values across the outcomes; see appendix C for details. Table 2 summarizes the results.

Table 2: UK Biobank: platelet global null

Resolution	Number of rejections			SNPs implicated		
	KeLP	Outer-nodes	Res. spec.	KeLP	Outer-nodes	Res. spec.
single-SNP	116	0	0	116	0	0
3 kb	77	96	96	783	954	954
20 kb	286	354	438	7,162	8,446	10,531
41 kb	143	146	539	5,003	5,123	19,010
81 kb	528	534	1,071	28,597	28,959	57,813
208 kb	334	334	1,268	30,815	30,815	123,340
425 kb	207	207	1,275	28,816	28,816	204,169
Total	1,691	1,671		101,292	103,113	

See caption of Table 1 for detailed explanations.

It is interesting to remark that KeLP can increase power for higher levels of resolutions compared to the standard “resolution specific” analysis. Indeed, the rejections by KeLP are not necessarily a subset of the outer-nodes of these. KeLP considers all hypotheses in the multi-resolution family jointly, which can result in a different threshold required for self-consistency than a resolution-specific threshold; see equation (6). The fact that a number of low resolution hypotheses are discovered, can then lower the threshold for high resolution ones to enter the rejection set.

8 Conclusion

We developed a method to localize signals at the smallest level of resolution possible while controlling frequentist FDR leveraging the concept of e-values. In particular, we focused on relaxed multi-resolution e-values from the knockoff filter. We have shown that our method can be used to parse over groups of features or groups of outcomes. Our method showed desirable performance in simulations and in an application to the UK Biobank. It successfully navigated the tradeoff between resolution and power, adaptively choosing a level of resolution that enables discoveries while maximizing their precision and controlling FDR.

The rejections of KeLP are not necessarily a subset of the outer-nodes of resolution-specific knockoffs filters. Indeed, by looking simultaneously across resolutions, and allowing discoveries of different levels of precision, KeLP can lead to a larger number of high resolution discoveries.

We observed in our experiments that KeLP achieves an empirical FDR that is usually lower than the target level. This might be connected to the self-consistency requirement, which, as stated in section 3, implicitly estimates the number of false discoveries as a fraction of all tested hypotheses, even though our non-redundancy requirement could never result in these

many rejections. The investigation of sharper bounds that would result in higher power might be the object of future work. Another possible direction for future research is to investigate whether logical constraints could be utilized for higher power, similar to [Meijer and Goeman \(2015\)](#) or [Ramdas et al. \(2019a\)](#).

Our results include methods to test conditional independence partial conjunction hypotheses using the same sample and a new version of the multilayer knockoff filter. All together, they underscore the versatility of e-values and provide examples where the technical elegance of this methodology is accompanied by substantial power.

References

- Barber, R. F. and Candès, E. J. (2015) Controlling the false discovery rate via knockoffs. *The Annals of Statistics*, **43**, 2055–2085.
- Barber, R. F. and Ramdas, A. (2017) The p-filter: multilayer false discovery rate control for grouped hypotheses. *Journal of the Royal Statistical Society: Series B (Statistical Methodology)*, **79**, 1247–1268.
- Benjamini, Y. and Heller, R. (2008) Screening for partial conjunction hypotheses. *Biometrics*, **64**, 1215–1222.
- Benjamini, Y. and Hochberg, Y. (1995) Controlling the False Discovery Rate: A Practical and Powerful Approach to Multiple Testing. *Journal of the Royal Statistical Society: Series B (Statistical Methodology)*, **57**, 289–300.
- Benjamini, Y. and Yekutieli, D. (2001a) The control of the false discovery rate in multiple testing under dependency. *Annals of Statistics*, 1165–1188.
- (2001b) The Control of the False Discovery Rate in Multiple Testing under Dependency. *The Annals of Statistics*, **29**, 1165–1188.
- Blanchard, G. and Roquain, E. (2008) Two simple sufficient conditions for FDR control. *Electronic Journal of Statistics*, **2**, 963–992.
- Bogomolov, M. and Heller, R. (2013) Discovering findings that replicate from a primary study of high dimension to a follow-up study. *Journal of the American Statistical Association*, **108**, 1480–1492.
- (2018) Assessing replicability of findings across two studies of multiple features. *Biometrika*, **105**, 505–516.
- Candès, E. J., Fan, Y., Janson, L. and Lv, J. (2018) Panning for gold: model-X knockoffs for high-dimensional controlled variable selection. *Journal of the Royal Statistical Society: Series B (Statistical Methodology)*, **80**, 551–577.
- Chu, B. (2023) Variable Selection with Knockoffs. <https://github.com/biona001/Knockoffs.jl>.
- Cortes, A., Dendrou, C. A., Motyer, A., Jostins, L., Vukcevic, D., Dilthey, A., Donnelly, P., Leslie, S., Fugger, L. and McVean, G. (2017) Bayesian analysis of genetic association across tree-structured routine healthcare data in the UK Biobank. *Nature Genetics*, **49**, 1311–1318.

- Dai, R. and Barber, R. (2016) The knockoff filter for fdr control in group-sparse and multitask regression. In *Proceedings of The 33rd International Conference on Machine Learning* (eds. M. F. Balcan and K. Q. Weinberger), vol. 48 of *Proceedings of Machine Learning Research*, 1851–1859. New York, New York, USA: PMLR. URL: <https://proceedings.mlr.press/v48/daia16.html>.
- Fu, A., Narasimhan, B. and Boyd, S. (2020) CVXR: An R package for disciplined convex optimization. *Journal of Statistical Software*, **94**, 1–34.
- Genovese, C. and Wasserman, L. (2004) A stochastic process approach to false discovery control. *Annals of Statistics*, **32**, 1035–1061.
- Gimenez, J. R., Ghorbani, A. and Zou, J. (2019) Knockoffs for the mass: new feature importance statistics with false discovery guarantees. In *The 22nd International Conference on Artificial Intelligence and Statistics*, 2125–2133. PMLR.
- Goeman, J. J., Meijer, R. J., Krebs, T. J. and Solari, A. (2019) Simultaneous control of all false discovery proportions in large-scale multiple hypothesis testing. *Biometrika*, **106**, 841–856.
- Goeman, J. J. and Solari, A. (2011) Multiple Testing for Exploratory Research. *Statistical Science*, **26**, 584 – 597.
- Grünwald, P., de Heide, R. and Koolen, W. (2020) Safe testing. *arXiv preprint arXiv:1906.07801*.
- Katsevich, E. and Sabatti, C. (2019) Multilayer knockoff filter: Controlled variable selection at multiple resolutions. *The Annals of Applied Statistics*, **13**, 1–33.
- Katsevich, E., Sabatti, C. and Bogomolov, M. (2021) Filtering the rejection set while preserving false discovery rate control. *Journal of the American Statistical Association*, 1–12.
- Li, S., Sesia, M., Romano, Y., Candès, E. and Sabatti, C. (2022) Searching for robust associations with a multi-environment knockoff filter. *Biometrika*, **109**, 611–629.
- Makhorin, A. (2008) Glpk (gnu linear programming kit). <http://www.gnu.org/s/glpk/glpk.html>.
- Mandozzi, J. and Bühlmann, P. (2016) Hierarchical testing in the high-dimensional setting with correlated variables. *Journal of the American Statistical Association*, **111**, 331–343.
- Meijer, R. J. and Goeman, J. J. (2015) A multiple testing method for hypotheses structured in a directed acyclic graph. *Biometrical Journal*, **57**, 123–143.
- Ramdas, A., Chen, J., Wainwright, M. J. and Jordan, M. I. (2019a) A sequential algorithm for false discovery rate control on directed acyclic graphs. *Biometrika*, **106**, 69–86.

- Ramdas, A. K., Barber, R. F., Wainwright, M. J. and Jordan, M. I. (2019b) A unified treatment of multiple testing with prior knowledge using the p-filter. *The Annals of Statistics*, **47**, 2790–2821.
- Ren, Z. and Barber, R. F. (2023) Derandomized knockoffs: leveraging e-values for false discovery rate control. *arXiv preprint arXiv:2205.15461*.
- Renaux, C., Buzdugan, L., Kalisch, M. and Bühlmann, P. (2020) Hierarchical inference for genome-wide association studies: a view on methodology with software. *Computational Statistics*, **35**, 1–40.
- Romano, Y., Sesia, M. and Candès, E. (2020) Deep knockoffs. *Journal of the American Statistical Association*, **115**, 1861–1872.
- Rosenblatt, J. D., Finos, L., Weeda, W. D., Solari, A. and Goeman, J. J. (2018) All-Resolutions Inference for brain imaging. *NeuroImage*, **181**.
- Sesia, M., Bates, S., Candès, E., Marchini, J. and Sabatti, C. (2021) False discovery rate control in genome-wide association studies with population structure. *Proceedings of the National Academy of Sciences*, **118**, e2105841118.
- Sesia, M., Katsevich, E., Bates, S., Candès, E. and Sabatti, C. (2020) Multi-resolution localization of causal variants across the genome. *Nature Communications*, **11**, 1–10.
- Sesia, M., Sabatti, C. and Candès, E. J. (2019) Gene hunting with hidden markov model knockoffs. *Biometrika*, **106**, 1–18.
- Shafer, G. (2021) Testing by betting: a strategy for statistical and scientific communication. *Journal of the Royal Statistical Society: Series A (Statistics in Society)*, **184**, 407–478.
- Simes, R. J. (1986) An improved Bonferroni procedure for multiple tests of significance. *Biometrika*, **73**, 751–754.
- Spector, A. and Janson, L. (2022) Powerful knockoffs via minimizing reconstructability. *The Annals of Statistics*, **50**, 252–276.
- (2023) Controlled Discovery and Localization of Signals via Bayesian Linear Programming. *arXiv preprint arXiv:2203.17208*.
- Theussl, S., Hornik, K., Buchta, C., Schwendinger, F., Schuchardt, H. and Theussl, M. S. (2019) Package ‘rglpc’. *GitHub, Inc., San Francisco, CA, USA, Tech. Rep. 0.6-4*.
- Vovk, V. and Wang, R. (2021) E-values: Calibration, combination and applications. *The Annals of Statistics*, **49**, 1736–1754.
- (2023) Confidence and discoveries with e-values. *Statistical Science*, **38**, 329–354.

- Wang, R. and Ramdas, A. (2022) False discovery rate control with e-values. *Journal of the Royal Statistical Society: Series B (Statistical Methodology)*, **84**, 822–852.
- Yekutieli, D. (2008) Hierarchical false discovery rate–controlling methodology. *Journal of the American Statistical Association*, **103**, 309–316.
- Yengo, L., Vedantam, S., Marouli, E., Sidorenko, J., Bartell, E., Sakaue, S., Graff, M., Eliassen, A. U., Jiang, Y., Raghavan, S. et al. (2022) A saturated map of common genetic variants associated with human height. *Nature*, **610**, 704–712.

A Proof of Theorem 1

Proof. The proof is essentially identical to the proof of proposition 2 in Wang and Ramdas (2022), but is included for completeness.

Let \mathcal{F} be a self-consistent e-testing procedure and $\mathbf{e} = (e_1, \dots, e_n)$ be an arbitrary vector relaxed e-variables satisfying $\sum_{j: H_j \in \mathcal{H}_0} \mathbb{E}[e_j] \leq n$.

This first part is identical to the proof of proposition 2 in Wang and Ramdas (2022):

$$\begin{aligned} \text{FDP}(\mathcal{F}) &= \frac{|\mathcal{F}(\mathbf{e}) \cap \mathcal{H}_0|}{R_{\mathcal{F}} \vee 1} \\ &= \sum_{j: H_j \in \mathcal{H}_0} \frac{\mathbf{1}\{j \in \mathcal{F}(\mathbf{e})\}}{R_{\mathcal{F}} \vee 1} \\ &\leq \sum_{j: H_j \in \mathcal{H}_0} \frac{\mathbf{1}\{j \in \mathcal{F}(\mathbf{e})\} \alpha e_j}{n} \\ &\leq \sum_{j: H_j \in \mathcal{H}_0} \frac{\alpha e_j}{n} \end{aligned}$$

Further following Wang and Ramdas (2022), but using knockoff e-values we get:

$$\begin{aligned} \text{FDR}(\mathcal{F}) &= \mathbb{E} \left[\frac{|\mathcal{F}(\mathbf{e}) \cap \mathcal{H}_0|}{R_{\mathcal{F}} \vee 1} \right] \\ &\leq \mathbb{E} \left[\sum_{j: H_j \in \mathcal{H}_0} \frac{\alpha e_j}{n} \right] \\ &= \frac{\alpha}{n} \sum_{j: H_j \in \mathcal{H}_0} \mathbb{E} [e_j] \\ &\leq \alpha \end{aligned}$$

The only change to the proof in Wang and Ramdas (2022) is the last inequality. Here, the last inequality is because $\sum_{j: H_j \in \mathcal{H}_0} \mathbb{E}[e_j] \leq n$ by assumption. □

B Focused e-BH vs eLP

Following Katsevich et al. (2021), let $\mathcal{R} \subseteq \mathcal{H}$ denote a collection of rejections from a multiple comparison procedure. Further, let \mathfrak{F} be a filter, a function that selects some elements of the

rejection set (according to their level of interest, for example, or to ensure non redundancy):
 $\mathfrak{F} : (\mathcal{R}, \mathbf{e}) \mapsto \mathcal{U} \subseteq \mathcal{H}$ with $\mathcal{U} \subseteq \mathcal{R}$.

We then define:

Algorithm S.1: Focused e-BH

Input: Vector of e-values $\mathbf{e} = (e_1, \dots, e_{|\mathcal{A}|})$, filter \mathfrak{F} .

Output: Filtered rejection set \mathcal{U}^*

for $t \in \{e_1, \dots, e_{|\mathcal{A}|}, \infty\}$ **do**

 | Compute $t \times |\mathfrak{F}(\{A \in \mathcal{A} : e_A \geq t\}, \mathbf{e})| \vee 1$

end

$t^* \leftarrow \inf \left\{ t \in \{e_1, \dots, e_{|\mathcal{A}|}, \infty\} : t \times |\mathfrak{F}(\{A \in \mathcal{A} : e_A \geq t\}, \mathbf{e})| \geq |\mathcal{A}|/\alpha \right\}$;

Find the base rejection set $\mathcal{R}^* = \{A : e_A \geq t^*\}$;

Compute $\mathcal{U}^* = \mathfrak{F}(\mathcal{R}^*, \mathbf{e})$

This algorithm fulfills self-consistency by definition and hence controls the FDR at level α without making any assumptions on the dependence among test statistics, structure of hypotheses or form of filter, as alluded to in Wang and Ramdas (2022). In contrast, the analogous Focused BH procedure by Katsevich et al. (2021) controls FDR when the filter fulfills some monotonicity requirements and/or the p-values are PRDS. While Katsevich et al. (2021) also use reshaping (Benjamini and Yekutieli, 2001a) to define a version of the procedure that is valid more generally, the resulting rejection set is conservative.

It is interesting to note that there is a close connection between eLP and Focused e-BH. For example, consider a multiresolution family of hypotheses defined by nested partitions, so that logical relations between hypotheses can be described by a tree. Further, consider two procedures: eLP with weights $w(A)$ decreasing in group size $|A|$ and Focused e-BH with the outer-nodes filter, which selects the rejections in \mathcal{R} that are not parent to any other rejection. Let \mathcal{R}_{on} be the output of Focused e-BH with the outer-nodes filter: \mathcal{R}_{on} is non-redundant by definition; moreover, by focusing on the outer-nodes, \mathcal{R}_{on} also selects the rejections with highest weight $w(A)$ among redundant sets, which is the goal of eLP. The two procedures, then, lead to the same set of rejections.

The outer-nodes filter is one example of a filtering procedure that can be described as a weighted maximization problem subject to constraints. Focused e-BH in combination with these filters results in the same set of rejections as eLP (where the constraints and weights for eLP could possibly be modified from Procedure 1). Below, we focus on filters with a non-redundancy constraint, as this is one of the main motivating observations in Katsevich et al. (2021).

Consider the for-loop in the Focused e-BH procedure (Algorithm S.1) and the definition of eLP (Procedure 1). We can write the inside of the for-loop as a maximization problem. For any $t \in \{e_1, \dots, e_{|\mathcal{A}|}, \infty\}$, applying a filter that can be described as a weighted maximization

problem with a non-redundancy constraint is equivalent to

$$\max_{\{x_A\}_{A \in \mathcal{A}}} \sum_{A \in \mathcal{A}} w(A)x_A \quad (\text{S.1a})$$

$$\text{subject to } x_A \in \{0, 1\} \quad \forall A \in \mathcal{A} \quad (\text{S.1b})$$

$$e_A \times x_A \geq t \times x_A \quad \forall A \in \mathcal{A}, \quad (\text{S.1c})$$

$$\sum_{A \in \mathcal{A}: j \in A} x_A \leq 1 \quad \forall j \in \{1, \dots, p\}, \quad (\text{S.1d})$$

Here, constraint (S.1c) does not control FDR, but ensures to only reject hypotheses with e-values $e_A \geq t$. Under the constraint that every rejected e-value fulfills $e_A \geq t$ and that the rejections are non-redundant (S.1d), the objective in (S.1a) maximizes the sum of weights of the rejected groups. For example, consider the outer-nodes filter: among all sets of groups $A \in \mathcal{A}$ with $e_A \geq t$ that would fulfill non-redundancy (S.1d), the outer-nodes maximize $\sum_{A \in \mathcal{A}} w(A)x_A$ by definition.

Next, consider choosing t^* (e.g. with the outer-nodes filter for nested groups of hypotheses) in the Focused e-BH procedure. By definition, this chooses the largest number of rejections, controlling the FDR; see algorithm S.1. Suppose that eLP and Focused e-BH were to choose two different thresholds, say $t^* = t_{\text{F-eBH}} < t_{\text{eLP}}$, which both control the FDR and fulfill the non-redundancy constraint. The objective of eLP (7a) is similarly to maximize the number of weighted rejections. Thus, we can achieve at least the same objective (7a) with $t_{\text{F-eBH}}$ compared to t_{eLP} . Therefore, choosing t^* means that (7a) is maximized as well.

While there exist more filters than those that can be described by eLP, the combination of a weighted maximization problem subject to a non-redundancy constraint is a constructive way to describe meaningful filters. For example, it allows to generalize the notion of the outer-nodes filter to non-nested partitions. In addition, eLP can be more computationally efficient than Focused BH, which loops through every possible input e-value.

C Partial conjunctions

For simplicity, consider first the case of a single level of resolution. We will therefore drop the subscript m indicating the resolution $m \in \mathcal{M}$ in the following.

Suppose that there are L outcomes and consider $L \geq 1$ conditional independence hypotheses of the form

$$H_0^\ell(A) : Y_\ell \perp\!\!\!\perp X_A \mid X_{-A} \text{ versus } H_1^\ell(A) : Y_\ell \not\perp\!\!\!\perp X_A \mid X_{-A} \quad (\text{S.2})$$

for each $\ell \in \{1, \dots, L\}$ and each $A \in \mathcal{A}$. For simplicity of notation, we will refer to the hypothesis tested at location A as H_A^ℓ . Further, let $\mathcal{H}_0^\ell = \{H_A^\ell : H_0^\ell(A) \text{ is true}\}$ be the outcome-specific set of true null hypotheses.

Let $v(A) \in \{1, \dots, L\}$ denote the number of false conditional independence nulls (S.2) at location $A \in \mathcal{A}$. Following [Benjamini and Heller \(2008\)](#), we are interested in testing

$$H_0^{u/L}(A) : v(A) < u \text{ versus } H_1^{u/L}(A) : v(A) \geq u \quad (\text{S.3})$$

for each $u \in \{1, \dots, L\}$ and each $A \in \mathcal{A}$. We will refer to the partial conjunction hypothesis tested at location A as $H_A^{u/L}$. Further, let $\mathcal{H}_0^{u/L} = \{H_A^{u/L} : H_0^{u/L}(A) \text{ is true}\}$ be the set of true partial conjunction nulls. For example, if $u = 1$, we are testing the global null hypothesis that a particular group $A \in \mathcal{A}$ is not conditionally associated to *any* outcome.

We will first consider testing (S.3) with regular e-values in section C.1. In section C.2 we consider e-values from the knockoff filter and discuss how to use them with KeLP.

C.1 Partial conjunctions with regular e-values

Consider testing (S.3) with regular e-values, as defined in section 3. The argument below closely follows [Benjamini and Heller \(2008\)](#). We start by discussing how to combine L regular e-values for outcome-specific hypotheses H_A^ℓ , $\ell \in \{1, \dots, L\}$, for group $A \in \mathcal{A}$ to obtain a valid partial conjunction e-value for group $A \in \mathcal{A}$.

Following [Benjamini and Heller \(2008\)](#), consider a vector of L outcome-specific e-values at a specific location A where the partial conjunction null holds, that is $A \in \mathcal{H}_0^{u/L}$. Further, for such a vector of e-values, let the first $1, \dots, L - u + 1$ e-values correspond to those where the outcome-specific null hypotheses are true. Then, let U_1, \dots, U_{L-u+1} be e-values for $i \in \{1, \dots, L - u + 1\}$ and let e_1, \dots, e_{u-1} be the other e-values. Let $e^{u/L} = f(U_1, \dots, U_{L-u+1}, e_1, \dots, e_{u-1})$ be the e-value for the partial conjunction hypotheses using a combining method f . As long as f is nondecreasing in all components,

$$f(U_1, \dots, U_{L-u+1}, h_1(e_1), \dots, h_{u-1}(e_{u-1})) \geq f(U_1, \dots, U_{L-u+1}, e_1, \dots, e_{u-1})$$

will hold for functions $h_i(x) \geq x$, $i = 1, \dots, u - 1$.

Lemma S.1. *Under $H_0^{u/L}(A)$, let $h_i(e_i) \geq e_i$ for some function $h_i(\cdot)$, $i = 1, \dots, u - 1$ and let*

$$\begin{aligned} e_*^{u/L}(A) &= f(U_1, \dots, U_{L-u+1}, h_1(e_1), \dots, h_{u-1}(e_{u-1})) \\ e^{u/L}(A) &= f(U_1, \dots, U_{L-u+1}, e_1, \dots, e_{u-1}) \end{aligned}$$

for a function f nondecreasing in all components. Then $e_*^{u/L}(A) \succeq e^{u/L}(A)$.

Let $x \in [0, \infty]$ and define $\infty \geq \infty$. If the event $\{e^{u/L}(A) \geq x\}$ occurs, then the event $\{f(U_1, \dots, U_{L-u+1}, h_1(e_1), \dots, h_{u-1}(e_{u-1})) \geq x\}$ occurs, which proves the lemma as in [Benjamini and Heller \(2008\)](#).

Using the argument in [Benjamini and Heller \(2008\)](#), under $H_0^{u/L}(A)$, the random variable $e^{u/L}(A) = f(U_1, \dots, U_{L-u+1}, e_1, \dots, e_{u-1})$ with fixed U_1, \dots, U_{L-u+1} satisfying $E(U_i) \leq 1$, is stochastically largest when each of the variables e_1, \dots, e_{u-1} is ∞ with probability one. Hence, we would like to make sure that in this case $\mathbb{E}[e_*^{u/L}(A)] \leq 1$, since then $1 \geq \mathbb{E}[e_*^{u/L}(A)] \geq \mathbb{E}[e^{u/L}(A)]$.

If $e_*^{u/L}(A)$ depends only on the $L - u + 1$ smallest e-values, for example by taking the average of the smallest $L - u + 1$ e-values, we would obtain $1 \geq \mathbb{E}[e_*^{u/L}(A)]$.

The pooled e-value would then be valid if it uses a combination function that satisfies:

$$\mathbb{E}[f(U_1, \dots, U_{L-u+1}, \infty, \dots, \infty)] \leq 1$$

In summary, for regular e-values, we could just take the average of the smallest $L - u + 1$ e-values to test the partial conjunction hypothesis at a group A .

Intuitively, this matches the result of [Benjamini and Heller \(2008\)](#) for p-values, who focus on the largest $L - u + 1$ p-values to find partial conjunction p-values. While other e-value combination methods could also be applied, such as a Simes e-value, we choose the arithmetic mean since it essentially dominates any symmetric e-merging function for the global null as shown by [Vovk and Wang \(2021\)](#). Note also that the average e-value is an e-value regardless of the dependency structure between the e-values by linearity of expectation; see also [Vovk and Wang \(2021\)](#).

The partial conjunction e-values stemming from regular e-values discussed in this section can be directly used in eLP; see section 3. We next discuss how to construct partial conjunction e-values based on the knockoff filter.

C.2 Partial conjunction hypotheses with knockoff e-values

We first show that partial conjunction e-values derived from the knockoff filter are not strictly e-values in the sense that the expected value under the null is bounded by 1 for every individual partial conjunction e-value, but instead fulfill a more relaxed condition. Then we consider how to use these knockoff partial conjunction e-values in KeLP.

To derive conditions for partial conjunction e-values from the knockoff filter, for simplicity of notation, we first focus on a single level of resolution in theorem S.2. We therefore first drop the subscript indicating the level of resolution - as such, in theorem S.2, c replaces c_m in equation (12).

Theorem S.2. *Given a single-resolution partition \mathcal{A} , we consider the set of partial conjunction hypotheses $\mathcal{H}^{u/L}$ as a family of hypotheses addressed by KeLP. We assume that valid e_A^ℓ fulfilling the conditions described in Procedure 2 are available for every $A \in \mathcal{A}$ and any $\ell \in \{1, \dots, L\}$. For any $A \in \mathcal{A}$, let $\bar{e}_A^{u/L} := \frac{1}{L-u+1} \sum_{i=1}^{L-u+1} e_A^{[u-1+i]}$, where $e_A^{[1]}, \dots, e_A^{[L]}$ denote the sorted knockoff e-values from largest to smallest. Let c denote the fixed multiplier as in the definition of knockoff e-values in equation (12). Then these partial conjunction e-values fulfill*

$$\sum_{A: H_A^{u/L} \in \mathcal{H}_0^{u/L}} \mathbb{E}[\bar{e}_A^{u/L}] \leq c \times \frac{L}{L-u+1}$$

Proof. First, consider the case where $u = 1$. Recall that by section 4, for each outcome $\ell \in \{1, \dots, L\}$, the knockoff e-values fulfill $\sum_{A: H_A^\ell \in \mathcal{H}_0^\ell} E[e_A^\ell] \leq c$. Then

$$\begin{aligned} \sum_{A: H_A^{u/L} \in \mathcal{H}_0^{u/L}} \mathbb{E}[\bar{e}_A^{u/L}] &= \sum_{A: H_A^{u/L} \in \mathcal{H}_0^{u/L}} \mathbb{E}\left[\frac{1}{L} \sum_{\ell=1}^L e_A^\ell\right] \\ &= \frac{1}{L} \sum_{\ell=1}^L \sum_{A: H_A^{u/L} \in \mathcal{H}_0^{u/L}} \mathbb{E}[e_A^\ell] \\ &\leq \frac{1}{L} \sum_{\ell=1}^L \sum_{A: H_A^\ell \in \mathcal{H}_0^\ell} \mathbb{E}[e_A^\ell] \\ &\leq \frac{1}{L} \sum_{\ell=1}^L c \\ &= c \end{aligned}$$

The first inequality follows as $\mathcal{H}_0^{u/L} \subseteq \mathcal{H}_0^\ell$ for each $\ell \in \{1, \dots, L\}$. Note that if $H_A^{u/L} \in \mathcal{H}_0^{u/L}$, then $v(A) = 0$ and $H_A^\ell \in \mathcal{H}_0^\ell$ for every $\ell \in \{1, \dots, L\}$. However, $H_A^\ell \in \mathcal{H}_0^\ell$ does not imply that $H_A^{u/L} \in \mathcal{H}_0^{u/L}$ if $v(A) \geq 1$ for at least one $\ell \in \{1, \dots, L\}$. The last inequality follows since $\sum_{A: H_A^\ell \in \mathcal{H}_0^\ell} \mathbb{E}[e_A^\ell] \leq c$ by construction of the knockoff e-values.

Next, consider the case that $u > 1$. The following two observations are crucial here: (1) For every $A : H_A^{u/L} \in \mathcal{H}_0^{u/L}$, the outcomes $\ell \in \{1, \dots, L\}$ corresponding to the $L-u+1$ considered e-values might be different. (2) The condition $\sum_{A: H_A^\ell \in \mathcal{H}_0^\ell} E[e_A^\ell] \leq c$ holds for every outcome separately.

As observation (2) concerns the sum over the expected null e-values for any outcome $\ell \in \{1, \dots, L\}$, it could happen, separately for each outcome $\ell \in \{1, \dots, L\}$, that $\mathbb{E}[e_{A'}^\ell] = c$ for some $A' : H_{A'}^\ell \in \mathcal{H}_0^\ell$, which implies that $\sum_{A: H_A^\ell \in \mathcal{H}_0^\ell \setminus H_{A'}^\ell} \mathbb{E}[e_A^\ell] = 0$.

Recall that as we only consider a single level of resolution for simplicity here, we let \mathcal{A} denote the partition of $\{1, \dots, p\}$ into disjoint groups. With $A_g \in \mathcal{A}$ for $g \in \{1, \dots, |\mathcal{A}|\}$ we indicate the elements of the partition \mathcal{A} , each of which is a disjoint set of indices $j \in \{1, \dots, p\}$. This partition \mathcal{A} is the same for every outcome $\ell \in \{1, \dots, L\}$. Below we find it helpful to consider different groups for different outcomes $\ell \in \{1, \dots, L\}$. These groups will be denoted by $A_{g^\ell} \in \mathcal{A}$.

Based on the discussion above, consider the case that for every $\ell \in \{1, \dots, L\}$ there is such a group $A'_{g^\ell} \in \mathcal{A}$ with $H_{A'_{g^\ell}}^\ell \in \mathcal{H}_0^\ell$ where $\mathbb{E}[e_{A'_{g^\ell}}^\ell] = c$.

First suppose that $A'_g = A'_{g_1} = \dots = A'_{g_L}$ for $A'_g \in \mathcal{A}$. As such, there is a single location $A'_g \in \mathcal{A}$ where for every $\ell \in \{1, \dots, L\}$, $H_{A'_g}^\ell \in \mathcal{H}_0^\ell$ and $\mathbb{E}[e_{A'_g}^\ell] = c$. Suppose that A'_g is also part of a partial conjunction null: $H_{A'_g}^{u/L} \in \mathcal{H}_0^{u/L}$. By construction of the partial conjunction e-values, this implies that $\bar{e}_{A'_g}^{u/L} = c$. Recall that for each outcome $\ell \in \{1, \dots, L\}$ there can be only a single location A'_{g^ℓ} with $\mathbb{E}[e_{A'_{g^\ell}}^\ell] = c$ for $H_{A'_{g^\ell}}^\ell \in \mathcal{H}_0^\ell$, which implies that $\sum_{A_{g^\ell}: H_{A_{g^\ell}}^\ell \in \mathcal{H}_0^\ell \setminus H_{A'_{g^\ell}}^\ell} \mathbb{E}[e_{A_{g^\ell}}^\ell] = 0$. Therefore, $\sum_{A: H_A^{u/L} \in \mathcal{H}_0^{u/L}} \mathbb{E}[\bar{e}_A^{u/L}] \leq c$ is still fulfilled in this case.

Next, consider the case that $A'_{g_1} \neq \dots \neq A'_{g_L}$. This means that the locations $A'_{g^\ell} \in \mathcal{A}$ with $H_{A'_{g^\ell}}^\ell \in \mathcal{H}_0^\ell$ and $\mathbb{E}[e_{A'_{g^\ell}}^\ell] = c$ are different for every $\ell \in \{1, \dots, L\}$.

Recall observation (1) and suppose that the partial conjunction null is true at every location $A'_{g_1}, \dots, A'_{g_L}$, i.e. $\{H_{A'_{g_1}}^{u/L}, \dots, H_{A'_{g_L}}^{u/L}\} \subseteq \mathcal{H}_0^{u/L}$. By the same logic as above, we obtain that $\bar{e}_{A'_{g_1}}^{u/L} = \dots = \bar{e}_{A'_{g_L}}^{u/L} = c \times \frac{1}{L-u+1}$.

As there can be at most one group A'_{g^ℓ} with $\mathbb{E}[e_{A'_{g^\ell}}^\ell] = c$ for every $\ell \in \{1, \dots, L\}$, we can bound $\sum_{A: H_A^{u/L} \in \mathcal{H}_0^{u/L}} \mathbb{E}[\bar{e}_A^{u/L}] \leq \min \left\{ c \times \left(\frac{L}{L-u+1} \right), c \times \left(\frac{c}{L-u+1} \right) \right\}$. In most applications $c \geq L$. Either way, we can always apply the following bound:

$$\sum_{A: H_A^{u/L} \in \mathcal{H}_0^{u/L}} \mathbb{E}[\bar{e}_A^{u/L}] \leq c \times \frac{L}{L-u+1}$$

□

In order to obtain FDR control with partial conjunction e-values with KeLP, it would be required that $\sum_{A: H_A^{u/L} \in \mathcal{H}_0^{u/L}} \mathbb{E} \left[\bar{e}_A^{u/L} \right] \leq |\mathcal{A}|$; see section 4. By theorem S.2, for FDR control it is therefore required that $c \times [L/(L - u + 1)] \leq |\mathcal{A}|$. Expressed differently, if only $c \leq |\mathcal{A}|$ is ensured, then FDR would not be controlled at level α , but instead at level $\alpha \frac{L}{L-u+1}$.

We next extend the previous result for a single level of resolution to multiple levels of resolution.

Procedure S.1. (KeLP with partial conjunction e-values) *Let $\mathcal{H}^{u/L}$ be a multi-resolution family of partial conjunction hypotheses addressed with KeLP. For each resolution $m \in \mathcal{M}$ and for each outcome $\ell \in \{1, \dots, L\}$, construct (group) knockoffs as defined in section 4 and obtain the corresponding e-value $e_{A_g^m}^\ell$ for every $A_g^m \in \mathcal{A}^m$ and every $\ell \in \{1, \dots, L\}$ as in Procedure 2, letting $\{c_m\}_{m \in \mathcal{M}}$ be non negative numbers such that $\frac{L}{L-u+1} \sum_{m \in \mathcal{M}} c_m \leq |\mathcal{A}|$. Then, within each level of resolution $m \in \mathcal{M}$, construct a partial conjunction e-value $\bar{e}_{A_g^m}^{u/L}$ for every $A_g^m \in \mathcal{A}^m$ as described in theorem S.2. For a fixed weighting function $w(\cdot)$, and a target FDR level α the rejection set of KeLP with partial conjunction e-values is given by the output of eLP (Procedure 1) taking the partial conjunction e-values as input.*

At each level of resolution separately, the partial conjunction e-values fulfill the property that

$$\sum_{A_g^m: H_g^{m, u/L} \in \mathcal{H}_0^{u/L, m}} \mathbb{E} \left[\bar{e}_{A_g^m}^{u/L} \right] \leq c_m \frac{L}{L - u + 1}.$$

Across all resolutions, this implies that

$$\sum_{m \in \mathcal{M}} \sum_{A_g^m: H_g^{u/L, m} \in \mathcal{H}_0^{u/L, m}} \mathbb{E} \left[\bar{e}_{A_g^m}^{u/L} \right] \leq \frac{L}{L - u + 1} \sum_{m \in \mathcal{M}} c_m.$$

By theorem 1 and the same argument as in section 4, for FDR control at level α it is therefore required to set c_m such that

$$\frac{L}{L - u + 1} \sum_{m \in \mathcal{M}} c_m \leq |\mathcal{A}|.$$

Alternatively, if it is only ensured that $\sum_{m \in \mathcal{M}} c_m \leq |\mathcal{A}|$, the FDR would only be controlled at level $\alpha \frac{L}{L-u+1}$.

However, note that in practice this adjustment factor ($L/(L - u + 1)$) for knockoff e-values might not be needed, as the existence of groups A where the partial conjunction null holds

with $\mathbb{E}[e_A^\ell] = c$ and $A \in \mathcal{H}_0^\ell$ (which implies that $\mathbb{E}[e_{A'}^\ell] = 0$ for all other $A' \in \mathcal{H}_0^\ell \setminus A$) that are distinct across $\ell \in \{1, \dots, L\}$ seems rather unlikely.

D e-Filter and e-MKF

D.1 Description

The p-filter by [Barber and Ramdas \(2017\)](#) coordinates rejections across partitions and controls the FDR simultaneously for all partitions. The original p-filter by [Barber and Ramdas \(2017\)](#) has been extended to arbitrary dependencies between the p-values in [Ramdas et al. \(2019b\)](#) using reshaping, which makes the procedure conservative. As mentioned in [Wang and Ramdas \(2022\)](#), it is possible to develop an analog of the p-filter for e-values.

The notation follows [Barber and Ramdas \(2017\)](#) and [Wang and Ramdas \(2022\)](#). Suppose that we have n regular, individual-level e-values $\mathbf{e} = (e_1, \dots, e_n)$ corresponding to hypotheses H_1, \dots, H_n and an unknown set of nulls \mathcal{H}_0 . Suppose that the hypotheses are organized into $|\mathcal{M}|$ different layers, where each layer consists of an arbitrary partition of the hypotheses into groups. Note that we are leaving the setting described in section 1. The hypotheses can be arbitrary and the e-values $\mathbf{e} = (e_1, \dots, e_n)$ do not have to correspond to features, which is why we will use the index notation $i \in \{1, \dots, n\}$ as opposed to $j \in \{1, \dots, p\}$. Moreover, the partitions do not have to be resolutions. We will return to the previous setting based on knockoff e-values and contiguous groups of different sizes with the same feature basis at the end of this section.

We use the arithmetic mean to combine e-values within each group as it dominates the analogue of Simes ([Simes, 1986](#)) for e-values ([Vovk and Wang, 2021](#)). However, if other group-level e-values are already available, these can be used instead as well. At the end of this section, we describe how to coordinate discoveries by the knockoff filter based on group-level knockoff e-values. As before, let $A_g^m \in \mathcal{A}^m$ for $g \in \{1, \dots, |\mathcal{A}^m|\}$ be the set of indices $i \in \{1, \dots, n\}$ belonging to group A_g^m .

We define $\infty \times \text{constant} = \infty$ and $\infty \geq \infty$. In this section, we consider regular e-values as defined in section 3. Note that by definition, e-values can take on the value ∞ ; see [Vovk and Wang \(2021\)](#). However, in the context of knockoff e-values, as described in section 4, ∞ is not a possible value.

We follow the notation and problem setup in [Barber and Ramdas \(2017\)](#). Consider thresholds $(t_1, \dots, t_{|\mathcal{M}|}) \in [0, \infty]^{|\mathcal{M}|}$. Assume for now that the thresholds are given, following [Barber and Ramdas \(2017\)](#), we will show below how to define these thresholds. Define the set of all discoveries that are made by the algorithm as:

$$\mathcal{R}(t_1, \dots, t_{|\mathcal{M}|}) := \{i : \text{for all } m, \text{Mean}(e_{A_g^m(i)}) \geq t_m\},$$

where $g(i)$ is the index of the group that e_i belongs to in partition m . Thus, a hypothesis i is selected if at every layer m , its group $A_{g(i)}^m$ has $\text{Mean}(e_{A_{g(i)}^m}) \geq t_m$.

Correspondingly, the rejection set at layer m is defined as

$$\mathcal{R}_m(t_1, \dots, t_{|\mathcal{M}|}) := \{A_g^m \in \mathcal{A}^m : \mathcal{R}(t_1, \dots, t_{|\mathcal{M}|}) \cap A_g^m \neq \emptyset\}.$$

Further define:

$$\tilde{\mathcal{R}}_m(t_1, \dots, t_{|\mathcal{M}|}) := |\mathcal{R}_m(t_1, \dots, t_{|\mathcal{M}|})| \vee 1$$

Following [Barber and Ramdas \(2017\)](#), let

$$\hat{\mathcal{T}}(\alpha_1, \dots, \alpha_{|\mathcal{M}|}) := \{(t_1, \dots, t_{|\mathcal{M}|}) \in [0, \infty]^{|\mathcal{M}|} : t_m \tilde{\mathcal{R}}_m(t_1, \dots, t_{|\mathcal{M}|}) \geq |\mathcal{A}^m|/\alpha_m \text{ for all } m\} \quad (\text{S.4})$$

where $\alpha_1, \dots, \alpha_{|\mathcal{M}|} \in [0, 1]$ is the desired level of FDR control for each layer m . Note that this ensures that the FDR is controlled at each level m by self-consistency; see [theorem 1](#). An alternative proof is included below [theorem S.4](#).

Continuing with the argument in [Barber and Ramdas \(2017\)](#), we let

$$\hat{t}_m := \min\{t_m \in [0, \infty] : \exists t_1, \dots, t_{m-1}, t_{m+1}, \dots, t_{|\mathcal{M}|} \text{ such that } (t_1, \dots, t_{|\mathcal{M}|}) \in \hat{\mathcal{T}}(\alpha_1, \dots, \alpha_{|\mathcal{M}|})\} \quad (\text{S.5})$$

for each $m = 1, \dots, |\mathcal{M}|$.

Theorem S.3. Fix $\alpha_1, \dots, \alpha_m \in [0, 1]$ and a vector of e -values $\mathbf{e} \in [0, \infty]^n$. Then $(\hat{t}_1, \dots, \hat{t}_m) \in \hat{\mathcal{T}}(\alpha_1, \dots, \alpha_{|\mathcal{M}|})$.

The proof follows [Barber and Ramdas \(2017\)](#):

Proof. By definition of \hat{t}_m there is some $t_1^m, \dots, t_{m-1}^m, t_{m+1}^m, \dots, t_{|\mathcal{M}|}^m$ for each m such that

$$(t_1^m, \dots, t_{m-1}^m, \hat{t}_m, t_{m+1}^m, \dots, t_{|\mathcal{M}|}^m) \in \hat{\mathcal{T}}(\alpha_1, \dots, \alpha_{|\mathcal{M}|}).$$

Therefore

$$\mathcal{R}(t_1^m, \dots, t_{m-1}^m, \hat{t}_m, t_{m+1}^m, \dots, t_{|\mathcal{M}|}^m) \subseteq \mathcal{R}(\hat{t}_1, \dots, \hat{t}_{m-1}, \hat{t}_m, \hat{t}_{m+1}, \dots, \hat{t}_{|\mathcal{M}|})$$

because $\mathcal{R}(t_1, \dots, t_{|\mathcal{M}|})$ is a non-increasing function of $(t_1, \dots, t_{|\mathcal{M}|})$ and for each $m' \neq m$, $\hat{t}_{m'} \leq t_{m'}^m$.

By definition, $\hat{t}_m \tilde{\mathcal{R}}_m(\hat{t}_1^m, \dots, \hat{t}_{m-1}^m, \hat{t}_m, \hat{t}_{m+1}^m, \dots, \hat{t}_{|\mathcal{M}|}^m) \geq |\mathcal{A}^m|/\alpha_m$.

But by the above we have that

$$\tilde{\mathcal{R}}(t_1^m, \dots, t_{m-1}^m, \hat{t}_m, t_{m+1}^m, \dots, t_{|\mathcal{M}|}^m) \leq \tilde{\mathcal{R}}(\hat{t}_1, \dots, \hat{t}_{m-1}, \hat{t}_m, \hat{t}_{m+1}, \dots, \hat{t}_{|\mathcal{M}|})$$

So therefore, we have that

$$\begin{aligned} \hat{t}_m \tilde{\mathcal{R}}(\hat{t}_1, \dots, \hat{t}_{m-1}, \hat{t}_m, \hat{t}_{m+1}, \dots, \hat{t}_{|\mathcal{M}|}) &\geq \hat{t}_m \tilde{\mathcal{R}}(t_1^m, \dots, t_{m-1}^m, \hat{t}_m, t_{m+1}^m, \dots, t_{|\mathcal{M}|}^m) \\ &\geq |\mathcal{A}^m|/\alpha_m \end{aligned}$$

Since this holds for all m , this shows that $(\hat{t}_1, \dots, \hat{t}_m) \in \hat{\mathcal{T}}(\alpha_1, \dots, \alpha_{|\mathcal{M}|})$ by definition of $\hat{\mathcal{T}}(\alpha_1, \dots, \alpha_{|\mathcal{M}|})$. □

Theorem S.4. *Let $(\hat{t}_1, \dots, \hat{t}_m)$ as above. Then, for each $m = 1, \dots, |\mathcal{M}|$ the method controls the FDR for the m -th partition,*

$$\mathbb{E}[FDP_m(\hat{t}_1, \dots, \hat{t}_{|\mathcal{M}|})] \leq \alpha_m \frac{|\mathcal{H}_0^m|}{|\mathcal{A}^m|}.$$

Proof. As with the corresponding p-value thresholds, $t_1, \dots, t_{|\mathcal{M}|}$ take values in

$$\hat{t}_m \in \left\{ \left\{ \frac{1}{\alpha_m} \frac{|\mathcal{A}^m|}{k} : k = 1, \dots, |\mathcal{A}^m| \right\} \cup \{\infty\} \right\}.$$

Fix any partition m . We will show FDR control separately for the case $\hat{t}_m = \infty$ and $\hat{t}_m < \infty$.

First suppose that $\hat{t}_m = \infty$.

Let $e_{A,avg}^m$ denote the average of the individual-level e-values for a particular group A_g^m . If $A_g^m \in \mathcal{R}_m(\hat{t}_1, \dots, \hat{t}_{|\mathcal{M}|})$, then we must have $e_{A,avg}^m \geq \hat{t}_m$.

Fix any $A_g^m : H_g^m \in \mathcal{H}_0^m$. If $\hat{t}_m = \infty$, then $\mathbf{1}\{A_g^m \in \mathcal{R}_m(\hat{t}_1, \dots, \hat{t}_{|\mathcal{M}|})\} = 0$ for any $A_g^m : H_g^m \in \mathcal{H}_0^m$ almost surely.

This is because we know that $\mathbb{E}[e_{A_g^m}] \leq 1$ for all $A_g^m : H_g^m \in \mathcal{H}_0^m$. However, this implies also that $e_{A_g^m} < \infty$ almost surely, because if ∞ was a possible value, then $\mathbb{E}[e_{A_g^m}] = \infty$, which cannot be true since $\mathbb{E}[e_{A_g^m}] \leq 1$.

Then

$$\begin{aligned} FDP_m(\hat{t}_1, \dots, \hat{t}_{m-1}, \infty, \hat{t}_{m+1}, \dots, \hat{t}_{|\mathcal{M}|}) &= \frac{|\mathcal{R}_m(\hat{t}_1, \dots, \hat{t}_{|\mathcal{M}|}) \cap \mathcal{H}_0^m|}{1 \vee |\mathcal{R}_m(\hat{t}_1, \dots, \hat{t}_{|\mathcal{M}|})|} \\ &= \sum_{A_g^m : H_g^m \in \mathcal{H}_0^m} \frac{\mathbf{1}\{A_g^m \in \mathcal{R}_m(\hat{t}_1, \dots, \hat{t}_{|\mathcal{M}|})\}}{1 \vee |\mathcal{R}_m(\hat{t}_1, \dots, \hat{t}_{|\mathcal{M}|})|} \\ &= 0 \end{aligned}$$

And therefore we also have that

$$\begin{aligned} \mathbb{E}[FDP_m(\hat{t}_1, \dots, \hat{t}_{m-1}, \infty, \hat{t}_{m+1}, \dots, \hat{t}_{|\mathcal{M}|})] &= \mathbb{E}[0] \\ &= 0 \\ &\leq \alpha_m \frac{|\mathcal{H}_0^m|}{|\mathcal{A}^m|} \end{aligned}$$

Now suppose that $\hat{t}_m < \infty$.

The above argument implies that if $A_g^m \in \mathcal{R}_m(\hat{t}_1, \dots, \hat{t}_{|\mathcal{M}|})$ for some null group $A_g^m : H_g^m \in \mathcal{H}_0^m$, then we must have $\hat{t}_m < \infty$ almost surely. Moreover, since $\hat{t}_m < \infty$ by the construction above we have that $\hat{t}_m \in [\frac{1}{\alpha_m}, \frac{|\mathcal{A}^m|}{\alpha_m}]$, so $\hat{t}_m > 0$.

Moreover, note that $t_m R(t)/|\mathcal{A}^m|$ only has downside jumps and if $t_m = 0$ this becomes zero; see also [Wang and Ramdas \(2022\)](#). Therefore

$$\hat{t}_m \tilde{\mathcal{R}}_m(\hat{t}_1, \dots, \hat{t}_{|\mathcal{M}|}) = \frac{|\mathcal{A}^m|}{\alpha_m}$$

Thus,

$$\begin{aligned}
FDP_m(\hat{t}_1, \dots, \hat{t}_{|\mathcal{M}|}) &= \frac{|\mathcal{R}_m(\hat{t}_1, \dots, \hat{t}_{|\mathcal{M}|}) \cap \mathcal{H}_0^m|}{1 \vee |\mathcal{R}_m(\hat{t}_1, \dots, \hat{t}_{|\mathcal{M}|})|} \\
&= \frac{|\mathcal{R}_m(\hat{t}_1, \dots, \hat{t}_{|\mathcal{M}|}) \cap \mathcal{H}_0^m|}{\widetilde{\mathcal{R}}_m(\hat{t}_1, \dots, \hat{t}_{|\mathcal{M}|})} \\
&= \sum_{A_g^m: H_g^m \in \mathcal{H}_0^m} \frac{\mathbf{1}\{A_g^m \in \mathcal{R}_m(\hat{t}_1, \dots, \hat{t}_{|\mathcal{M}|})\}}{\widetilde{\mathcal{R}}_m(\hat{t}_1, \dots, \hat{t}_{|\mathcal{M}|})} \\
&\leq \alpha_m \frac{1}{|\mathcal{A}^m|} \hat{t}_m \sum_{A_g^m: H_g^m \in \mathcal{H}_0^m} \mathbf{1}\{A_g^m \in \mathcal{R}_m(\hat{t}_1, \dots, \hat{t}_{|\mathcal{M}|})\}
\end{aligned}$$

Fix any null group $A_g^m : H_g^m \in \mathcal{H}_0^m$. If A_g^m is selected, then we must have $e_{A,avg}^m \geq \hat{t}_m$.

Recall that A_g^m is a null group. Since $\mathbb{E}[e_i] \leq 1$ for each $i \in A_g^m$, we also have that $\mathbb{E}[e_{A,avg}^m] \leq 1$. Note also both $e_{A,avg}^m$ and \hat{t}_m are non-negative.

$$\begin{aligned}
FDP_m(\hat{t}_1, \dots, \hat{t}_{|\mathcal{M}|}) &\leq \alpha_m \frac{1}{|\mathcal{A}^m|} \hat{t}_m \sum_{A_g^m: H_g^m \in \mathcal{H}_0^m} \mathbf{1}\{A_g^m \in \mathcal{R}_m(\hat{t}_1, \dots, \hat{t}_{|\mathcal{M}|})\} \\
&= \alpha_m \frac{1}{|\mathcal{A}^m|} \hat{t}_m \sum_{A_g^m: H_g^m \in \mathcal{H}_0^m} \mathbf{1}\{e_{A,avg}^m \geq \hat{t}_m\}
\end{aligned}$$

Then, taking expectations we get that

$$\begin{aligned}
\mathbb{E}[FDP_m(\hat{t}_1, \dots, \hat{t}_{|\mathcal{M}|})] &\leq \alpha_m \frac{1}{|\mathcal{A}^m|} \sum_{A_g^m: H_g^m \in \mathcal{H}_0^m} \mathbb{E}[\hat{t}_m \mathbf{1}\{e_{A,avg}^m \geq \hat{t}_m\}] \\
&\leq \alpha_m \frac{1}{|\mathcal{A}^m|} \sum_{A_g^m: H_g^m \in \mathcal{H}_0^m} \mathbb{E}[e_{A,avg}^m] \\
&\leq \alpha_m \frac{1}{|\mathcal{A}^m|} \sum_{A_g^m: H_g^m \in \mathcal{H}_0^m} (1) \\
&\leq \alpha_m \frac{|\mathcal{H}_0^m|}{|\mathcal{A}^m|}
\end{aligned}$$

Hence, we get FDR control in either case: if $\hat{t}_m = \infty$ and if $\hat{t}_m < \infty$.

□

To find the thresholds \hat{t}_m , the algorithm in [Barber and Ramdas \(2017\)](#) can be adapted:

Algorithm S.2: Find thresholds \hat{t}_m , following [Barber and Ramdas \(2017\)](#)

Input: A vector of e-values $\mathbf{e} \in [0, \infty]^n$, target FDR levels $\alpha_1, \dots, \alpha_{|\mathcal{M}|}$, arbitrary partitions \mathcal{A}^m of the hypotheses into groups for each $m \in \mathcal{M}$

Output: Thresholds \hat{t}_m for $m \in \mathcal{M}$

Initialize: $t_1 \leftarrow 1/\alpha_1, \dots, t_{|\mathcal{M}|} \leftarrow 1/\alpha_{|\mathcal{M}|}$;

while $t_1, \dots, t_{|\mathcal{M}|}$ are all unchanged in the last round **do**

for $m = 1, \dots, |\mathcal{M}|$ **do**

 Define $\mathcal{R}_m(t_1, \dots, t_{|\mathcal{M}|}) = \{A_g^m \in \mathcal{A}^m\} : \mathcal{R}(t_1, \dots, t_{|\mathcal{M}|}) \cap A_g^m \neq \emptyset\}$ (as above);

$t_m \leftarrow \min\{\tilde{t} \in [t_m, \infty] : \tilde{\mathcal{R}}_m(t_1, \dots, t_{m-1}, \tilde{t}, t_{m+1}, \dots, t_{|\mathcal{M}|}) \geq |\mathcal{A}^m|/\alpha_m\}$

end

end

This construction can also be used to obtain a Multilayer Knockoff Filter inspired by [Katsevich and Sabatti \(2019\)](#) with valid FDR control at each level $m \in \mathcal{M}$. To do so, we define e-values as in section 4 to test the conditional independence hypothesis at each level of resolution for a single outcome. However, it is important to set $c_m = |\mathcal{A}^m|$ in order to obtain FDR control at each level $m \in \mathcal{M}$. This ensures that

$$\sum_{A_g^m: H_g^m \in \mathcal{H}_0^m} \mathbb{E}[e_{A_g^m}] \leq |\mathcal{A}^m|$$

holds at each level of resolution separately. As shown in theorem 1, this condition is sufficient to obtain FDR control in combination with self-consistency. As the thresholds $t_1, \dots, t_{|\mathcal{M}|}$ are obtained as described above; see equation (S.4), the knockoff e-value based multilayer knockoff filter also controls the FDR at each level $m \in \mathcal{M}$.

Note that as in section 4, W_m and T_m are defined separately for each layer. Moreover, the coordination of discoveries is conducted via the thresholds $t_1, \dots, t_{|\mathcal{M}|}$ (S.4). This is in contrast to [Katsevich and Sabatti \(2019\)](#), who coordinate the rejections in different layers directly via the knockoff stopping time (13) and control the FDR defined by the knockoff ([Candès et al., 2018](#); [Barber and Candès, 2015](#)). If we were to translate this procedure into e-values, the procedure by [Katsevich and Sabatti \(2019\)](#) would be based on

$$\tilde{e}_{A_g^m} = |\mathcal{A}^m| \cdot \frac{\mathbf{1}\{W_{A_g^m} \geq T_m^*\}}{1 + \sum_{A \in \mathcal{A}^m} \mathbf{1}\{W_A \leq -T_m^*\}} \quad (\text{S.6})$$

with T_m^* defined as in [Katsevich and Sabatti \(2019\)](#) in combination with the e-BH procedure at level α_m at each layer $m \in \mathcal{M}$. In equation (S.6), T_m^* not only depends on $m \in \mathcal{M}$, but

also on the other layers $m' \neq m \in \mathcal{M}$; see [Katsevich and Sabatti \(2019\)](#) for further details. The difficulty with using T_m^* dependent on other layers is that T_m^* cannot be represented as a stopping time that only depends on W_m anymore. This results in FDR control at level $\alpha_m \times \kappa$ instead of level α_m , where $\kappa \approx 1.93$.

D.2 Simulation

For comparability, we follow the simulation setting in [Katsevich and Sabatti \(2019\)](#) based on $M = 2$ layers. Layer 1 is comprised of individual variables and layer 2 of groups of size 10 (i.e. each group contains 10 individual variables).

We simulate data from a linear model $Y = X\beta + \epsilon$, where $\epsilon \sim \mathcal{N}(0, I)$ with $n = 4,500$ and $p = 2,000$. $X \in \mathbb{R}^{p \times n}$ is sampled independently from $\mathcal{N}(0, \Sigma_\rho)$ for $\rho = 0.3$ where $(\Sigma_\rho)_{ij} = \rho^{|i-j|}$ is the covariance of an AR(1) process with correlation ρ .

Following [Katsevich and Sabatti \(2019\)](#), we first select $r \in \{10, 20\}$ groups uniformly at random and then choose uniformly at random 75 elements of these r groups to determine the nonzero elements of β . The absolute value of the 75 non-zero elements β are determined by a/\sqrt{n} , where a denotes the signal amplitude, which is the parameter that we will vary. The sign of the non-zero coefficient is determined by independent coin flips. Following [Katsevich and Sabatti \(2019\)](#), we construct fixed-equi knockoff variables and choose lasso-based variable importance statistics combined using the signed-max function. We tune γ on an independently generated tuning data set with the same parameters and dimensions. Each point in the simulation results below is based on 100 iterations.

We compare the multilayer knockoff filter (MKF) with the knockoff e-value version (e-MKF) at the same theoretical guarantee of $\alpha_m = 0.2$ for both $m \in \{1, 2\}$. This shows that the e-MKF has higher power compared to the MKF for the same theoretical level of FDR control.

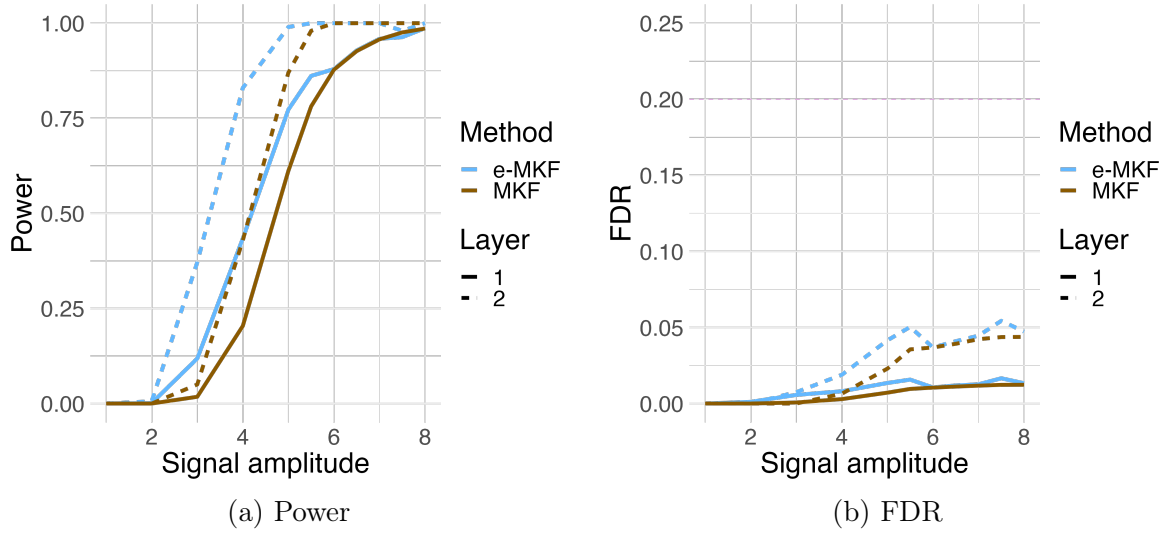


Figure 7: Number of nonzero groups: 10.

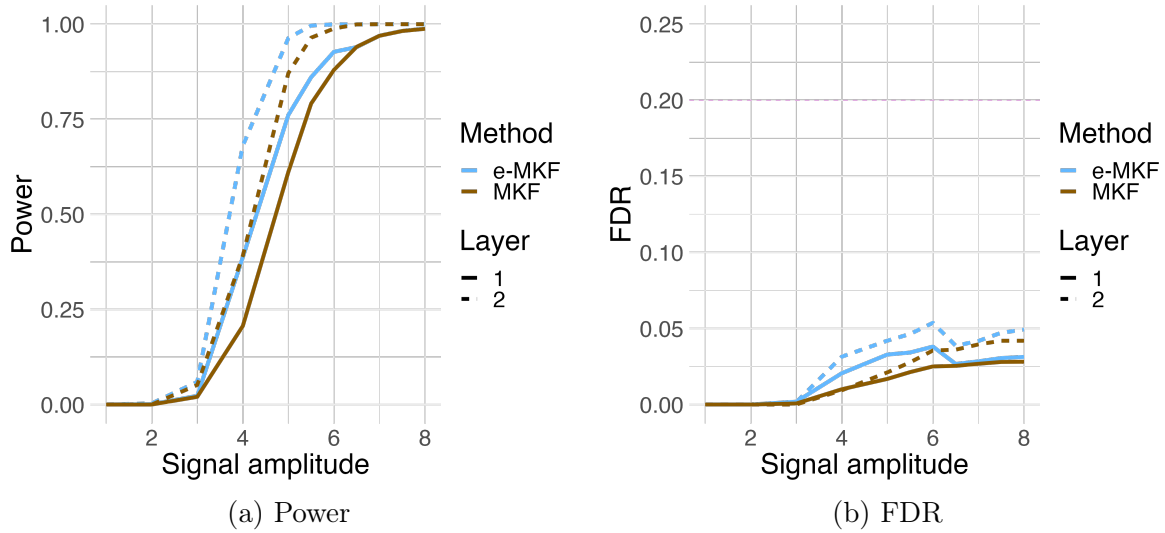


Figure 8: Number of nonzero groups: 20.

E Details on the simulations

We construct the knockoff e-values as in equation (12). In sections 6.1 and 6.3, the (group) knockoff variables are generated via maximum entropy (Spector and Janson, 2022; Chu, 2023).

Let $T_j = \beta_j$ and $\tilde{T}_j = \tilde{\beta}_j$ where β_j and $\tilde{\beta}_j$ are the coefficient estimates based on a 10-fold cross-validated lasso for variable j and its knockoff, respectively (Chu, 2023; Candès et al., 2018). Following Chu (2023), we compute $T_A = \sum_{j \in A} |T_j|$ and $\tilde{T}_A = \sum_{j \in A} |\tilde{T}_j|$ and set $W_A = T_A - \tilde{T}_A$ for each group $A \in \mathcal{A}$ to get the importance statistics.

For the chromosome-wide simulation on the UKB genotypes, we use the SHAPEIT knockoff variables by Sesia et al. (2021); see Sesia et al. (2021) for further details on pre-processing, importance statistics, knockoff variable generation and population definitions. As in Sesia et al. (2021), to obtain the importance statistics we run a cross-validated lasso including sex (data field 22001-0.0), age (data field 21003-0.0), squared age and the top five genetic principal components as covariates.

We set $c_m = |\mathcal{A}|/|\mathcal{M}|$, our default value, for each $m \in \mathcal{M}$ in all simulations. Following our default recommendations for γ discussed in section 4, we set $\gamma = \alpha/2$ for our simulations in section 6.1 and 6.3. In the more high-dimensional simulation on the UK Biobank genotypes of chromosome 21 in section 6.2, we set $\gamma = \alpha/4$.

Moreover, for the simulations in sections 6.1 and 6.3, following Spector and Janson (2023), the absolute value of each nonzero coefficient is set to be at least $0.1 \times \tau$, as otherwise there might be a few nonzero coefficients that are very close to zero.

Figure 9 shows $\text{Var}(f(X))/\text{Var}(Y) = \text{Var}(X\beta)/\text{Var}(X\beta + \epsilon)$ as a function of signal amplitude for the simulation setting of section 6.2.

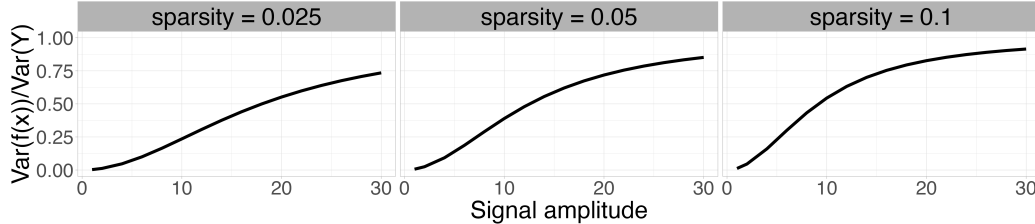


Figure 9: $\text{Var}(f(X))/\text{Var}(Y) = \text{Var}(X\beta)/\text{Var}(X\beta + \epsilon)$ for the chromosome-wide simulation on chromosome 21 of the UK Biobank. Different levels of sparsity by column. Other simulation details as in figure 5 in section 6.2.

Considering the structured outcome simulations in section 6.3 and the tree depicted in figure 3, for consistency with our previous simulations, we focus on the case where only the rejection of outcome A is reported at the leaf level (but not the rejection of $\{A, B\}$). Specifically, for simplicity, we leverage the connection between the Focused e-BH procedure and KeLP, which is further discussed in appendix B, for our simulations in section 6.3. Another option is to report both rejections with the argument that while A can be rejected at the leaf level, we

can only reject B at the level $\{A, B\}$. It is possible to adjust the location constraint in KeLP (7d) corresponding to either desired definition.

We solve the linear program corresponding to KeLP with CVXR (Fu et al., 2020) and the solver “Rglpk” (Theussl et al., 2019; Makhorin, 2008).

F Details on the UKB application

In all of our UK Biobank applications, we utilize the generated knockoff variables and the partitions by Sesia et al. (2021) based on UK Biobank application 27837. The around 592,000 SNPs are partitioned into contiguous groups at seven levels of resolution based on complete-linkage hierarchical clustering. The group sizes range from size one (single SNP) to 425-kb-wide groups; see Sesia et al. (2021) for further details on the UKB pre-processing, importance statistic, knockoff variable generation and population definitions. As Sesia et al. (2021), to obtain the importance statistics we run a cross-validated lasso including sex (data field 22001-0.0), age (data field 21003-0.0), squared age and the top five genetic principal components as covariates. Our outcomes of interest are height (data field 50-0.0), platelet count (data field 30080-0.0), platelet crit (data field 30090-0.0), platelet width (data field 30110-0.0) and platelet volume (data field 30100-0.0).

In this application with seven levels of resolution KeLP runs within minutes using CVXR (Fu et al., 2020) and the solver “Rglpk” (Theussl et al., 2019; Makhorin, 2008). For the majority of phenotypes considered the runtime is less than 5 minutes. KeLP for the outcome height has the longest runtime with about 20 minutes.

F.1 Additional results

F.1.1 Height: portion of genome implicated



Figure 10: Groups rejected by KeLP in each chromosome (1-11): height

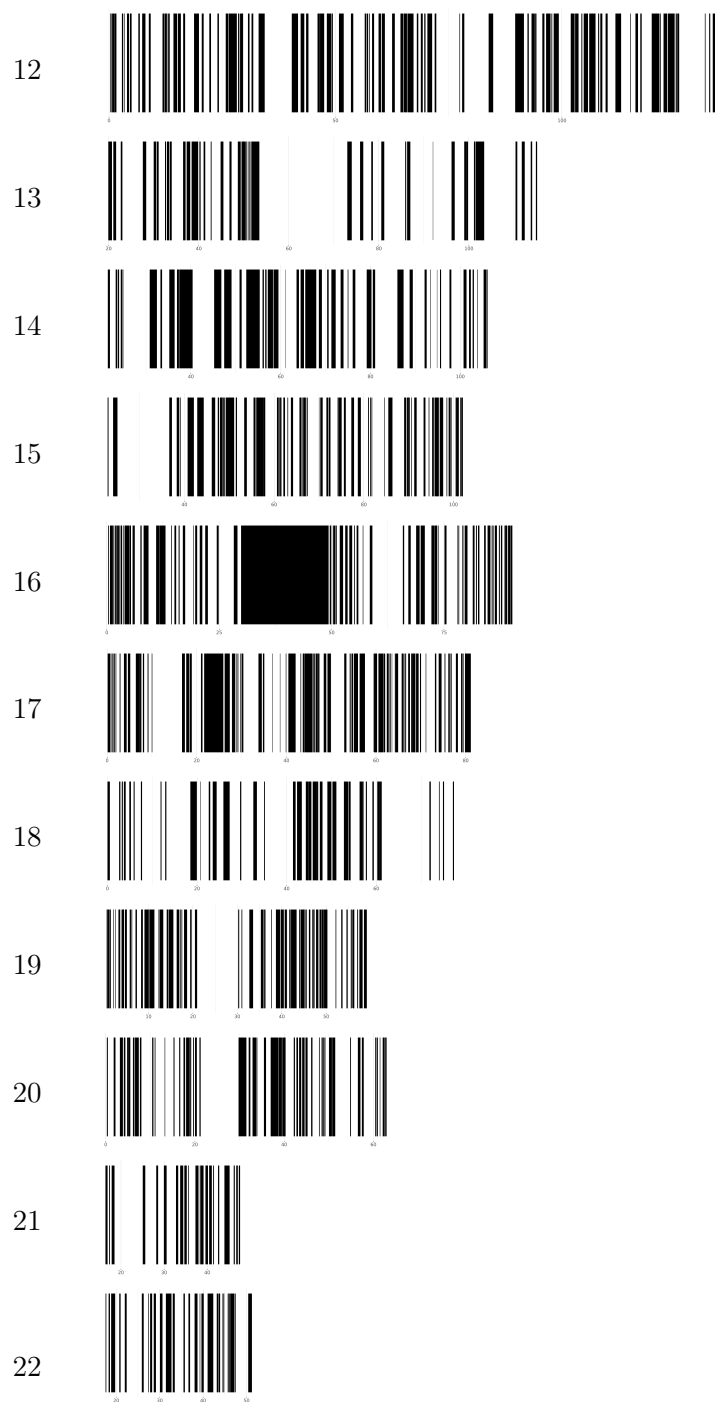


Figure 11: Groups rejected by KeLP in each chromosome (12-22): height

F.2 Defining e-value parameters for UK Biobank application

As discussed in section 4, we choose $c_m = \frac{|\mathcal{A}|}{|\mathcal{M}|}$ for each $m \in \mathcal{M}$. Since we are interested in KeLP on the unrelated British population, we use the unrelated White Non-British population as a separate tuning dataset to choose γ . The definition of populations follows from [Sesia et al. \(2021\)](#). Note that the White Non-British population has a much smaller number of observations compared to the British population, which is our population of interest (14,733 observations compared to 337,117 observations (i.e. less than 5% of the British sample size), indicating that a large tuning dataset might not be required.

Figure 12 displays the smallest γ resulting in a finite stopping time T_m on the White Non-British population for our outcomes of interest. These curves for the smallest γ displays two “dips” at the single-SNP and the 3 kb level. From group sizes starting at 20 kb the smallest γ does not exhibit much variation. We therefore choose γ to be resolution-dependant. As discussed in section 4, we deterministically set $\gamma = \alpha$ for the single-SNP level and $\gamma = \alpha/2$ on the 3 kb level. For the 20 kb level and up we tune γ on the White Non-British population. For simplicity, we will use the same γ for each level of resolution starting at 20 kb. For computational efficiency, we run e-BH on a set of pre-filtered groups, where the pre-filtering steps into the direction of KeLP: let a block denote a particular group in the coarsest level of resolution. Within each block, we filter to the group with the largest weight-adjusted fraction (where the weight is based on inverse group-size). We then run e-BH on this pre-filtered set of groups and choose the γ which results in the largest number of non-zero rejections across different α . If there are ties, we choose the larger γ .

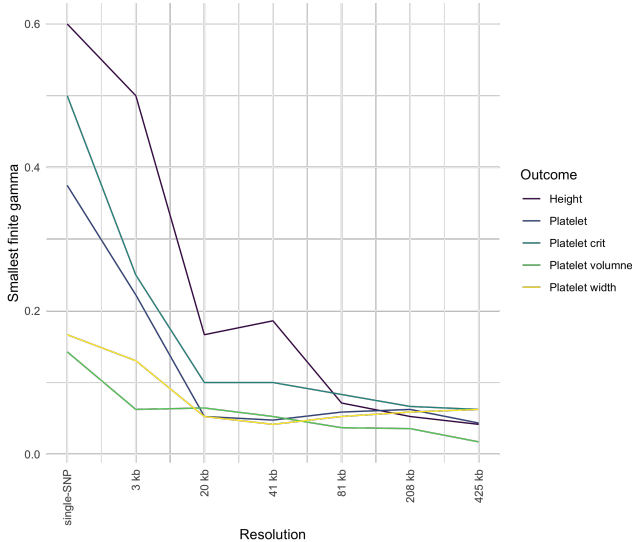


Figure 12: Smallest finite γ for White Non-British population by resolution.